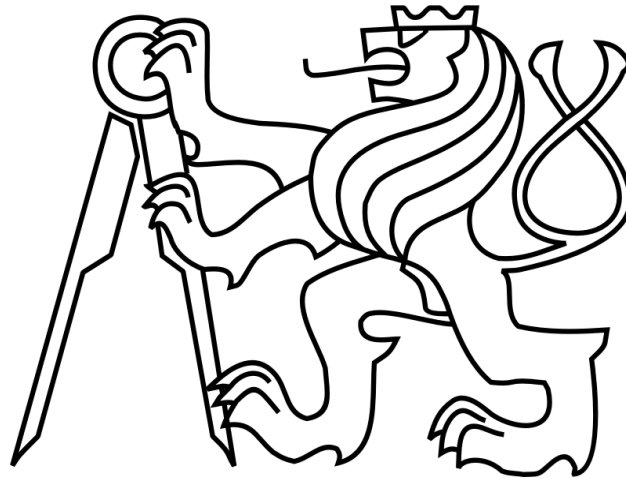# CZECH TECHNICAL UNIVERISTY IN PRAGUE
FACULTY OF ELECTRICAL ENGINEERING
DEPARTMENT OF PHYSICS

Runaway electrons

Master's thesis

Author: Martin Štencel
Supervisor: prof. RNDr. Petr Kulhánek, CSc.

Lausanne 2017

ZADÁNÍ DIPLOMOVÉ PRÁCE

ČESKÉ VYSOKÉ UČENÍ TECHNICKÉ V PRAZE

I. OSOBNÍ A STUDIJNÍ ÚDAJE

Příjmení: **Štencel**   Jméno: **Martin**   Osobní číslo: **399169**

Fakulta/ústav: **Fakulta elektrotechnická**

Zadávající katedra/ústav: **Katedra elektrotechnologie**

Studijní program: **Elektrotechnika, energetika a management**

Studijní obor: **Technologické systémy**

II. ÚDAJE K DIPLOMOVÉ PRÁCI

Název diplomové práce:

Ubíhající elektrony

Název diplomové práce anglicky:

Runaway electrons

Pokyny pro vypracování:

1) Diskutujte možné kanály rozpadů ubíhajících elektronů.
2) Dohledejte v dostupné literatuře dosud naměřené/vypočtené účinné průřezy jednotlivých reakcí.
3) Řešte numericky kreaci elektronových-pozitronových párů ubíhajícími elektrony za pomoci Monte Carlo metod.
4) Proveďte rozbor úniku energie tímto kanálem pro tokamak COMPASS.

Seznam doporučené literatury:

[1] Jan Mlynář: Some preliminary results from the first RE campaign on COMPASS; 2nd Chalmers meeting, 2014
[2] Ilen Boozer: Theory of runaway electrons in ITER: Equations, important parameters, and implications for mitigation; Physics of Plasmas 22, 032504 (2015)
[3] Ondřej Ficker: Generation, losses and detection of runaway electrons in tokamaks; Maszter's theses (2015), CTU Faculty of Nuclear Sciences and Physical Engineering

Jméno a pracoviště vedoucí(ho) diplomové práce:

prof. RNDr. Petr Kulhánek CSc.,   katedra fyziky   FEL

Jméno a pracoviště druhé(ho) vedoucí(ho) nebo konzultanta(ky) diplomové práce:

Datum zadání diplomové práce: **20.02.2017**   Termín odevzdání diplomové práce: **11.08.2017**

Platnost zadání diplomové práce: **07.09.2018**

_____   _____   _____
Podpis vedoucí(ho) práce   Podpis vedoucí(ho) ústavu/katedry   Podpis děkana(ky)

III. PŘEVZETÍ ZADÁNÍ

_____   _____
Datum převzetí zadání   Podpis studenta

Contents

Declaration

I acknowledge that I worked on this thesis independently and that I mentioned all information sources, which have been used according to Metodický pokyn č. 1/2009 about ethical principles related to preparation of final thesis.

Done in Prague on: ....

Bc. Martin Štencel

Acknowladgement

Abstract

This thesis focuses on the phenomenon of high energetic electrons in fusion and astrophysical plasma – so called runaway electrons. In the first part, the theoretical background is put forward. This includes the description of plasma, fusion reaction technologies as well as two of the main approaches used in plasma physics – microscopic and statistic. Using those two approaches, description of the runaway particles is put forward including their ways of formation, energy losing channels and possible ways of extinction. The second part includes the methodology and numerical approaches which are later used in the third part – the Monte Carlo numerical simulation. Its goal is to investigate one of the energy losing channels of runaway particles, which is electron-positron pairs generation. In this part, the algorithm itself is described. Then, the results of the simulation are discussed in the context of current knowledge.

Anotace

Tato práce se zabývá chováním vysokoenergetických elektronů ve fúzním a kosmickém plazmatu – tzv. ubíhajících (runaway) elektronů. V první, teoretické části práce je stručně popsáno plazma jako takové, současné fúzní technologie a dva z nejdůležitějších přístupů, jež jsou k popisu plazmatu používány – mikroskopický a statistický. Na nich je založen teoretický model ubíhajících elektronů včetně způsobů jejich vzniku, způsobů, kterými tyto elektrony ztrácejí energii a možností, jak mohou zanikat. Ve druhé části práce je popsána metodologie a numerické metody, které jsou následně použity ve třetí, praktické části práce, kterou je numerická Monte Carlo simulace. Jejím cílem je výpočet vlivu jednoho ze ztrátových kanálů runaway elektronů, kterým je generování elektronových-pozitronových párů těmito elektrony. Zde je posán samotný algoritmus výpočtu a jsou diskutovány výsledky simulace v kontextu současných poznatků z oblasti fyziky plazmatu.

Keywords

Plasma, tokamak, runaway particle, electron-positron pair, Monte Carlo simulation.

1. Introduction

There are more than 7 billion people on our planet. In order to satisfy their everyday needs, increasing amount of energy has to be produced. This production is obtained from number of sources. Some of them are polluting (coal, gas, oil), unstable (wind, solar), have limited possibilities of expansion (water, wind), low energy density resulting in problems with transport (coal, gas, oil) or there is an adverse political/social perception (nuclear fission) etc.

In spite of various advantages mentioned sources of energy can have, searching for stable, non-polluting and reliable source of energy seems to be inevitable. Probably the most promising candidate of the last few decades is thermonuclear fusion [1].
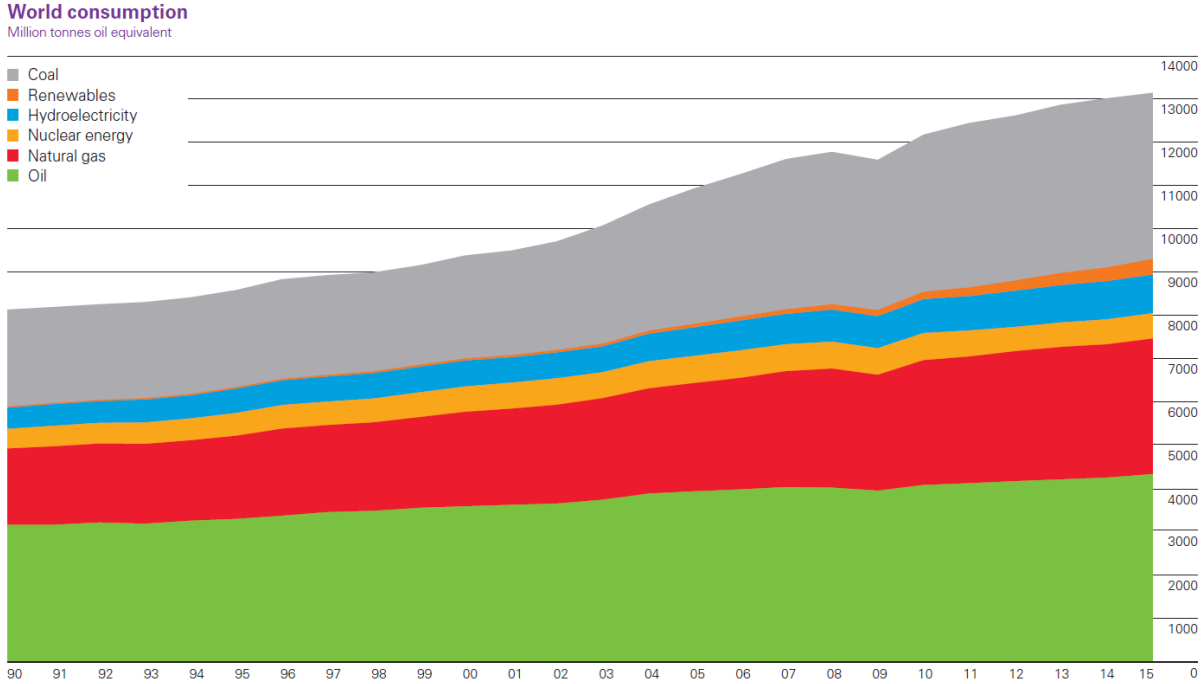

Figure 1: World energy consumption. Slightly increasing as mentioned [3].

2. Nuclear fusion

It is a well-known fact that the nuclear fusion is the mechanism by which our Sun is producing its energy while on the other hand fusion reaction cannot be found anywhere in nature on the Earth. The potential energy of nucleus is given by the rest mass of nucleus and it can be changed into kinetic energy by nuclear forces. Here we are using the fact that the average binding energy of nucleus is not constant with mass number. The difference in binding energy before and after the reaction means a difference in mass. The light elements have small binding energy per nucleon and hence large mass per nucleon. Therefore, fusion of such elements leads to the difference in mass after the reaction, which is proportional to huge amount of energy given by $\Delta E = \Delta mc^2$. On the other side of the curve we can find heavy elements. Here the energy can be released by fission, as the lighter products of decay have larger binding energy and hence smaller rest mass per nucleus. It is obvious from the Figure 1 that the nuclear fusion is much more effective than fission [4], [5].

Figure 2: Binding energy of nucleus per nucleon as a function of mass number [5].

Compared to nuclear fission, nuclear fusion is inherently safe, it produce no radioactive waste and moreover there is enough of fuel on the Earth for possibly billions of years. As another advantage, huge specific energy (Joules per kilogram of fuel) can be mentioned. The fusion also cannot be exploited for weapon production. However, the technology of fusion reaction is difficult to handle and the way towards a power plant based on this technology will be longer than ever before [1], [6].

As mentioned, all stars produce their energy by this mechanism and that is how light elements including iron were created. Heavier elements had to undergo supernova explosion, which

event can provide sufficient amount of temperature and pressure for creating elements as such. It has been also mentioned, that fusion reaction does not take place on the Earth. The reason is that the mechanism of the fusion requires two nuclei to get very close together – approximately 10^{-14} m. To make it happen, immense force is required because of repulsing Coulombic forces. Until 50s of previous century the only "devices" capable of providing such conditions were stars. In 1.11.1952 the first so called thermonuclear bomb was detonated by the USA army in the Pacific Ocean. Despite the fact that this event have started a new era of arms race and the thermonuclear bombs were being improved for many years, a peaceful use of this technology is still far from being implemented, facing number of problems. In order to get two nuclei close enough together, initiating the fusion reaction, we can either accelerated them and make them collide or we can heat them to proportional temperature. While the first option does not seem to be efficient, the second one is possible to perform. However, in this case the temperature is so high that no material can withstand in any other state than as plasma. So here comes the biggest problem: How to confine the hot plasma? Every known material evaporates when it comes to contact with such a hot matter like plasma is. Exact conditions are given by Lawson criterion. Here so called bremsstrahlung radiation is neglected and deuterium-tritium (D-T) reaction is considered (see below).

$$n_{\mathrm{e}}\tau_{\mathrm{e}} \geq \frac{10\,T}{\langle \sigma v \rangle_{\mathrm{DT}} \Delta E_{\mathrm{f}}}, \tag{1}$$

where n_{e} is a concentration of charged particles [m^{-3}], τ_{e} is a confinement time [s], T is temperature [eV], ΔE_{f} is energy of one reaction [eV], σ is a fusion cross-section [m^2] and v is a relative velocity between D and T. Finally, the symbol $< >_{\mathrm{DT}}$ denotes an average over the D and T distributions. The right side of the equation is a function of temperature with a local minimum as on the Figure 3. Typical values required for D-T reaction are $n_{\mathrm{e}}\tau_{\mathrm{e}} \geq 10^{20}$ m^{-3}s and $T \geq 10$ keV.

Note: It is usual in plasma physics that the temperature is expressed by electronvolts (eV) instead of kelvins using the equation $E = k_{\mathrm{B}}T$ where k_{B} is the Boltzmann constant and 1 eV $\sim 1.602 \cdot 10^{-19}$ J) [1], [6].

Figure 3: The Lawson criterion – break even condition for D-T reaction. Ignition condition indicates self-sustaining state of plasma (i.e. without any input power). Adapted from [1].

Now basically two approaches are feasible.

2.1 Inertial confinement – large n_e (~$10^{31}\,\mathrm{m}^{-3}$) and small τ_e ($10^{-11}\,\mathrm{s}$).

Here, the hot plasma is not confined and the reaction has to take place before the plasma expands to space, so this approach can be considered as a tiny thermonuclear bomb explosion. For this purpose cylindrical surface targets of mm size with enormous symmetry requirements are used. Source of energy are either laser beams or RTG radiation sources. Being imposed to energy source, the surface gives its energy to the fuel inside which results in steep increase in temperature initiating the nuclear fusion. As the most efficient sources of energy are the lasers, today's research is focused on development of sufficiently strong and cheap laser devices.

2.2 Magnetic confinement – small n_e (~10^{20} m^{-3}) and large τ_e (~1 s).

The fusion reaction with the lowest initiating temperature is the D-T reaction:

Plasma	$D + T \rightarrow {}^4He + n$	17.6 MeV
Tritium-breeding layer	${}^6Li + n \rightarrow {}^4He + T$	4.78 MeV
	${}^7Li + n \rightarrow {}^4He + T + n$	–2.47 MeV

Figure 4: The deuterium-lithium cycle with the reaction yields in the right column. Note that the tritium is bred right in the reactor. Adapted from [4].

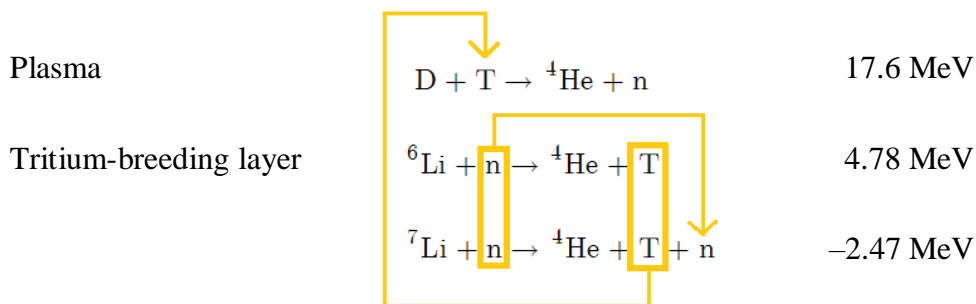Where the D – deuterium – can be found in the sea water as 1/6700 of its amount. T – tritium – is radio-active and short-lived element so it cannot be found in the nature. However, it can be bred right in the reactor according to Figure 4 using lithium layers in the walls of the confinement devices.

In this case outer magnetic field is used. The path of the charged particles is curved by this field into a circle around the direction of the magnetic field lines. The less of collisions there is and the stronger is the field, the better are the charged particles with their direction perpendicular to the field lines confined inside. On the other hand, the charged particles whose direction of motion is parallel with respect to the field lines are not influenced by the field anyhow. Devices capable of providing such configuration can be either opened (magnetic mirror) or closed (tokamak, stellarator, toroidal pinch). For this thesis we will deal with the tokamak as the tokamak concept has the best experimental results so far. Let us mention some record holders.

- Longest plasma duration time – Tore Supra, France – 6 minutes 30 seconds.
- Highest triple product (i.e. density, temperature, confinement time) – JT-60, Japan.
- Temperatures ~ millions of K in US devices [2].

Also for the biggest current project ITER, taking place in Cadarche in France, the technology is used. The tokamak might be capable of providing 500 MW of power with 50 MW of input power. However, it is still not a real power station, just a prototype of reactor. Not only the whole plasma physics community is looking up with hope to this project, which may be launched in 2025 [1], [4].

3. Tokamak

The word tokamak has its origin in Russian expression for toroidal chamber with magnetic coils. There is a toroidal magnetic field inside of the tokamak created by coils surrounding the tokamak chamber. The plasma is confined by this field, not touching the walls. To reach sufficient shape of the magnetic field lines, there is also a current inside the plasma itself. This current is delivered by induction from tokamak core, which plays a role of transformer's primary circuit while the plasma is the secondary circuit. Joule heating provided by the current is the main source of heat for the plasma. However, to reach sufficient temperature, at least another two heat sources have to be used – beam of neutral particles and microwaves in case of ITER [4], [6].
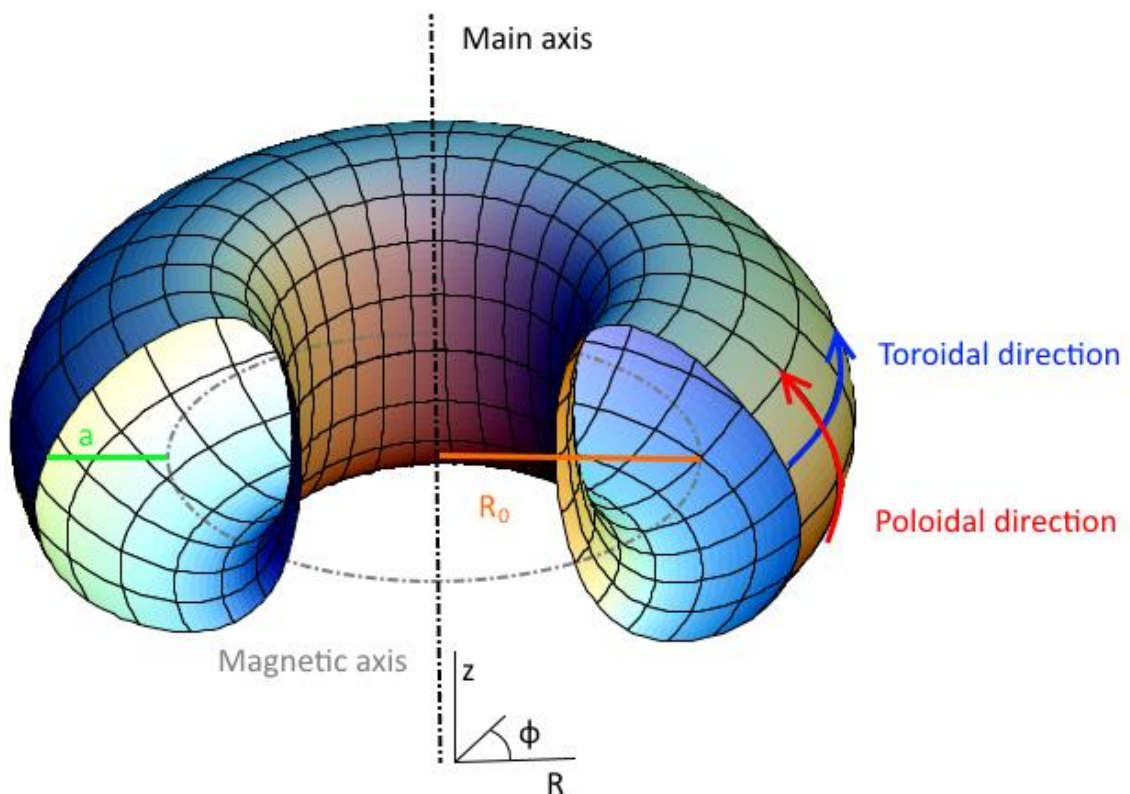

Figure 5: Tokamak cross-section. Here R_0 is the major radius and a the minor radius. Note that in fact the tokamak is not simple torus, but D-shape is used instead in order to improve stability of the plasma [6].

4. Plasma

We understand the concept of plasma as the fourth state of matter. The matter can be considered in plasma state if it satisfies these three following conditions.

- Presence of free charge carriers.

- Collective behaviour i.e. plasma exhibits collective response to the electric and magnetic field.

- Quasi-neutrality, meaning that the electric charge is zero in every macroscopic volume.

„The collective behaviour is possible because of the long range Coulomb interaction between the particles. Plasma interacts with external electromagnetic fields and the particles are affected by fields generated by other particles. Therefore, plasma is a self-consistent system and it is difficult to find numerical solution describing various processes in plasma."[6]
Plasma is the most common state of matter in our space. In fact, our Earth with its "normal" state of matter is sort of an oasis in a desert of the plasma. On the Earth, the plasma can be found in lightning, ionosphere or in the aurora. Also we use the plasma in many parts of industry e.g. dry etching, cutting, deposition of films etc. The most common mechanism of ionisation is the impact mechanism. As the temperature increases, free electrons have higher thermal energy. When such an electron collides with an atom, another electron can be released if the energy of the incoming electron is sufficiently high. Simultaneously with the ionisation process, there is also a recombination process taking place. In the case of the tokamak plasma, this process is mostly done by radiation. Here, the incoming electron is accepted by ion and energy in the form of a photon is radiated. The plasma is considered to be in equilibrium when those two processes are in the equilibrium [6], [7], [13].
The most important quantities to describe the plasma are electron concentration n_e and electron temperature T_e. Depending on the temperature, plasma can be either partially or fully ionised. It can be in the area of electron-positron pairs generation or not. Finally, for the highest temperatures, the plasma becomes relativistic. On the other hand, for the highest densities, the plasma exhibits quantum behaviour e.g. in the cores of the stars. There are many other possibilities of division of the plasma e.g. according to the thermal equilibrium, resistivity, collision frequency etc. Beside of the electrons, there are also ions, naturally. Those particles are described by the corresponding quantities n_i [m^{-3}] and T_i [eV]. Another two important values are the magnitude of the outer magnetic field B [T] and the plasma current I_p [A]. With these quantities, we can define three important frequencies to characterise the processes in the plasma.

$$\omega_{p\alpha}^2 = \frac{Q_\alpha^2 n_\alpha}{\varepsilon_0 m_\alpha}, \qquad \omega_{c\alpha} = \frac{Q_\alpha B}{m_\alpha}, \qquad \nu_{\alpha\beta} = \frac{n_e Q_\alpha^2 Q_\beta^2 \ln(\lambda)}{4\pi \varepsilon_0^2 m_e^2 c^3}, \qquad (2)$$

which corresponds to plasma frequency (frequency of plasma oscillations), cyclotron frequency (gyration around the vector of the magnetic field) and collisional frequency, respectively. Here the indices α and β corresponds to the incoming particle and the target particle. Q is the electric charge [C], ε_0 is the permittivity of the vacuum [F/m] and m is the mass of the particle [kg]. For every of these frequencies corresponding characteristic length can be defined.

$$\lambda_{\mathrm{D}}^2 = \frac{\varepsilon_0 k_{\mathrm{B}}}{\sum\limits_{\alpha} \dfrac{Q_\alpha^2 n_\alpha}{T_\alpha}}, \qquad\qquad r_{\mathrm{L}\alpha} = \frac{m_\alpha v_\perp}{Q_\alpha B}, \qquad\qquad \lambda_\alpha = \frac{v_{T\alpha}}{\nu_{\alpha\beta}}. \qquad (3)$$

Here, the first quantity is the Debye shielding length [m] with Boltzmann constant k_{B} [J/K]. In the vacuum, the potential of a charged particle decreases as $1/r$, while in the plasma, the particle is shielded by other particles resulting in decrease of its potential as $\exp(-r/\lambda_{\mathrm{D}})$Important is the number of particles N_{D} in a sphere with its radius equal to λ_{D}. If $N_{\mathrm{D}} \gg 1$, the collective effects prevail over the collision effects. Then we talk about ideal plasma. The left side of the second equation is so called Larmor radius [m] – a radius of a cyclic motion of a particle with a perpendicular component of velocity $v_\perp$ [m/s] around the magnetic field line. The last quantity is the mean free path of the particle [m], which is a function of thermal velocity $v_{T\alpha}$ [m/s] and the relative velocity between particles $v_{\alpha\beta}$ [m/s]. Here the mean free path is considered to be a mean distance between changing direction of motion of the particle by 90° [6], [7].

5. Relativistic particle motion in external fields

The RE have by definition very high energies, which can overcome their rest energy many times. Hence, non-relativistic description cannot be used. Let us start with the relativistic Lagrange function.

$$L = L_{\mathrm{p}} + L_{\mathrm{int}} = -m_0 c^2 \sqrt{1 - v^2 / c^2} - Q\phi + Q\mathbf{A}\cdot\mathbf{v}. \tag{4}$$

Here, L is the Lagrange function [J] which consists of the particle term L_{p} and the interaction term L_{int}, respectively. m_0 is the mass [kg], c is the speed of light in the vacuum [m/s], $\mathbf{v}$ is the velocity [m/s], ϕ is the scalar potential [V], and $\mathbf{A}$ is the vector potential [V·s·m^{-1}]. Obviously, for low velocities the equation can be considered to be equal to non-relativistic Lagrange function as the term v^2/c^2 goes to zero. If we introduce relativistic mass as

$$m \equiv \frac{m_0}{\sqrt{1 - v^2 / c^2}} = m_0\gamma, \tag{5}$$

where γ is the Lorentz factor [-], we can write energy and momentum in very compact form:

$$\mathbf{p} \equiv \frac{\partial L}{\partial \mathbf{v}} = m\mathbf{v} + Q\mathbf{A}, \qquad\qquad \varepsilon = \frac{\partial L}{\partial \mathbf{v}}\cdot\mathbf{v} - L = mc^2 + Q\phi. \tag{6}$$

After the Legendre dual transformation (i.e. replacement of velocity by momentum) the Hamilton function takes a form

$$H = c\sqrt{m_0 c^2 + (\mathbf{p} - Q\mathbf{A})^2} + Q\phi, \tag{7}$$

with potentials defined by following relations

$$\mathbf{B} = \nabla \times \mathbf{A}, \qquad\qquad \mathbf{E} = -\nabla\phi - \frac{\partial \mathbf{A}}{\partial t}. \tag{8}$$

From the Lagrangian (or Hamiltonian) we can derive the relativistic Lorentz equation of motion:

$$\frac{\mathrm{d}\mathbf{p}}{\mathrm{d}t} = Q(\mathbf{E} + \mathbf{v} \times \mathbf{B}). \tag{9}$$

The equation is relativistic because $\mathbf{p}$ depends on v^2/c^2. [6][7]
Let us also mention here the relation between total energy E and kinetic energy T in relativistic case [8]:

$$T = m_0\gamma c^2 - m_0 c^2, \qquad\qquad E = m_0\gamma c^2. \tag{10}$$

However, such an approach is not suitable for RE description as it does not contain any radiation term (i.e. reaction of a particle to its own field). This is crucial because the RE can lose their energy by radiation. Paul Dirac tried to figure out this problem and so in 1938 so called Lorentz-Dirac (LD) equation has been put forward [9][10].

$$\frac{\mathrm{d}P^\alpha}{\mathrm{d}\tau} = F_{\text{ext}}^\alpha + m\tau_0(g^\alpha{}_\beta + U^\alpha U_\beta)\frac{\mathrm{d}a^\beta}{\mathrm{d}\tau}. \tag{11}$$

With

$$P^\alpha = \begin{pmatrix} E/c \\ p_x \\ p_y \\ p_z \end{pmatrix}, \quad U^\alpha = \begin{pmatrix} \gamma_c \\ \gamma v_x \\ \gamma v_y \\ \gamma v_z \end{pmatrix}, \quad a^\alpha = \frac{\mathrm{d}U^\alpha}{\mathrm{d}\tau} \text{ and } \tau_0 \equiv \frac{\mu_0 e^2}{6\pi cm}, \tag{12}$$

which corresponds to four-momentum [kg·m·s^{-1}], four-velocity [m·s^{-1}], four-acceleration [m·s^{-2}] and preacceleration time [s] respectively. $g^\alpha{}_\beta$ is the metric matrix [m] and here it has the meaning of Kronecker delta, τ is so called proper time [s] and it is a Lorentz invariant. Finally, F_{ext}^α is an external force [N]. In this case, it is the standard Lorentz force

$$F_{\text{ext}}^\alpha = Q F^{\alpha\beta}U_\beta, \qquad\qquad F^{\mu\nu} \equiv \partial^\mu A^\nu - \partial^\nu A^\mu, \tag{13}$$

where $F^{\mu\nu}$ is the electromagnetic tensor [T]. The LD equation can be expressed in local Lorentz system of coordinates (an inertial system of coordinates which moves with the particle for a short time). Then we talk about Abraham-Lorentz-Dirac equation (ALD) [9], [10]:

$$m\mathbf{a} = \mathbf{F}_{\text{ext}} + m\tau_0\frac{\mathrm{d}\mathbf{a}}{\mathrm{d}\tau}. \tag{14}$$

Both LD and ALD equations have serious problems. First obvious problem is that for $\mathbf{F}_{\text{ext}} = 0$ we find an exponential solution i.e. the particle with zero initial velocity will be exponentially accelerated by its own field. This is not acceptable. The second problem is that for usual case of second-order differential equation, the initial condition consists of the particle's position and velocity. A third-order equation which we have here requires additional piece of initial information and it is not clear what it should be. Finally, the third problem is that the value of the force in presence depends on its value in the future – the causality principle is violated. Then meaning of the quantity τ_0 can be expressed as how far to the future the particle can "see" (fortunately not much as $\tau_0 \sim 10^{-24}$s). During nearly 80 years following the derivation of the LD equation, a lot of attempts to solve these problems have been put forward. For example it is possible to write the equation in integro-differential form [10].

$$\mathbf{a}(t) = \frac{1}{m}\int_0^\infty \mathbf{F}_{\text{ext}}(t + s\tau_0)\mathrm{e}^{-s}\mathrm{d}s. \tag{15}$$

However, the equation is not equivalent to (14). Only every solution of (15) is also solution of (14). Here, exponential solutions are suppressed but the problem with causality violence remains. In 2000, Michael Ibison and Harold E. Puthoff suggested a solution based on equation (15) when they found its integrating factor and they expand the solution into a series with τ_0 orders [11].

$$\frac{\mathrm{d}\mathbf{p}}{\mathrm{d}t} = \frac{1}{\gamma^3}\sum_{n=0}^{\infty}(\gamma\tau_0\frac{\mathrm{d}}{\mathrm{d}t})^n\gamma^2(\mathbf{F}_{\text{ext}}) - \frac{\mathbf{v}}{c}\left(\frac{\mathbf{v}}{c}\mathbf{F}_{\text{ext}}\right). \tag{16}$$

The series works very well for lower energies suppressing the non-physical solutions, but it diverges for energies of particle higher than its rest energy. In 2015 Alechandro Cabo Montes de Oca and Nana Geraldine Cabo Bizet suggested a modification, which might work also for ultrarelativistic energies. However, neither (16) nor (17) do not work for combined electric and magnetic fields [12].

$$ma^{\mu}(\tau) - f^{\mu}(\tau) = \kappa\left(\frac{\mathrm{d}}{\mathrm{d}t}a^{\mu}(\tau) + a^{\nu}(\tau)a_{\nu}(\tau)u^{\mu}(\tau)\right]$$

$$+\kappa\sum_{n=0}^{\infty}(a^{\nu}(\tau_n^-)\delta^{(D,-)}(\tau-\tau_n)$$

$$-a^{\mu}(\tau_n^+)\delta^{(D,-)}(\tau-\tau_n)). \tag{17}$$

Another interesting solution can be to find acceleration iteratively. If we assume the radiation term in the equation (14) negligible in the zero step, we can express the acceleration a_0 and use it for the first step [10].

$$m_0\mathbf{a}_1 = \mathbf{F}_{\text{ext}} + m_0\tau_0\frac{\mathrm{d}}{\mathrm{d}t}\frac{\mathbf{F}_{\text{ext}}}{m_0} \tag{18}$$

This approach is very popular, but the assumption about negligibility of radiation term can be problematic. According to some, better way how to deal with all the issue is to return back to the original Dirac's approach through the Maxwell tensor (i.e. momentum flux tensor). Here it would be necessary to make correction of the momentum loss by radiation in every step.
To mention something positive about LD equation, it gives correct solutions e.g. for energy balance and it is indeed the best we have [10], [13].

6. Statistical approach and the Fokker-Planck equation

In real plasma, it is typically impossible to describe every single particle with its equation of motion. The particles are simply too many. Therefore, in some cases it is advantageous to use statistical approach instead. One of the cases is RE. Then we are not given information about individual particles but about their mean behaviour and statistical distributions. The most basic term used in this approach is probability density of particle occurrence. It is defined in seven-dimensional phase space (instead of four-dimensional space as before in particle motion approach) and index α denotes the kind of the particle (electron, ion, neutral...).

$$f_\alpha = f_\alpha(t, \mathbf{x}, \mathbf{v}_\alpha). \tag{19}$$

Meaning of this quantity can be expressed as follows

$$\int f_\alpha(t, \mathbf{x}, \mathbf{v}_\alpha)\, \mathrm{d}^3 \mathbf{v}_\alpha = n_\alpha(t, \mathbf{x}), \tag{20}$$

$$\int f_\alpha(t, \mathbf{x}, \mathbf{v}_\alpha)\, \mathrm{d}^3 \mathbf{x}\, \mathrm{d}^3 \mathbf{v}_\alpha = N_\alpha(t). \tag{21}$$

We can notice that the probability is not standardised to 1 here, but to concentration of particles n_α [m^{-3}] instead. N_α is the number of particles α. Unit of the f_α is therefore [s^{3}m^{-6}]. The probability density of particle of type α occurrence can change in time due to collisional processes. This is expressed by the Boltzmann equation

$$\frac{\partial f_\alpha}{\partial t} + (\mathbf{v}_\alpha \cdot \nabla_{\mathbf{x}}) f_\alpha + \frac{1}{m_\alpha}(\mathbf{F}_\alpha \cdot \nabla_{\mathbf{v}}) f_\alpha = \sum_\beta S_{\alpha\beta}, \tag{22}$$

where the terms on the left side correspond to change in time t, space $\mathbf{x}(t)$ and velocity $\mathbf{v}(t)$ respectively. The term on the right side is so called Boltzmann collisional integral and it describes collisional effects among particles of various types. Solution of the Boltzmann equation then strongly depends on what assumptions we have for the $S_{\alpha\beta}$ term description. Being in the seven-dimensional space we have to distinguish between space gradient and velocity gradient. Other variables have standard meaning. In order to describe the RE we will use following assumptions about the collisional term.

- We observe the system for short time period Δt and during this period a change in velocity $\Delta \mathbf{v}$ is also small while a significant number of collisions take a place.

- We take into account pair and elastic collisions only.

- $b_0 \leq b \leq \lambda_{\mathrm{D}}$, where b is so called impact parameter [m] describing the Coulombic collision. b_0 is so called Landau parameter. It is a value of b for which the particle changes its direction by 90° after the collision. This means that we do not take into account frontal collisions. The reason is that in the case of the change of velocity direction by more than 90° the first assumption about small changes of velocity $\Delta \mathbf{v}$ would be violated. Such an assumption is reasonable as frontal collisions are not very

probable. Quantity λ_D is the shielding length from equation (3). As mentioned earlier, behind this boundary we consider the plasma particles unrecognizable.

- The field from other particles affecting one specific particle is a superposition of contributions from the particles inside the λ_D sphere.

- The collisions form the Markov chain (i.e. the process is ‚memoryless'). This also means that the probability of the velocity change $\Delta\mathbf{v}$ during Δt is not time depending.

Under these assumptions we can derive the Fokker-Planck equation – the equation (22) with the collisional term

$$S_{\alpha\beta} \equiv C_{\alpha\beta} \ln \Lambda_{\alpha\beta} \left[-\frac{m_\alpha + m_\beta}{m_\beta} \nabla_\mathbf{v} \cdot (f_\alpha \nabla_\mathbf{v} H_{\alpha\beta}) + \frac{1}{2}(\nabla_\mathbf{v} \nabla_\mathbf{v}) : (f_\alpha \nabla_\mathbf{v} \nabla_\mathbf{v} G_{\alpha\beta}) \right]. \quad (23)$$

With

$$H_{\alpha\beta}(\mathbf{v}_\alpha) \equiv \int \frac{1}{g} f_\beta \, \mathrm{d}^3\mathbf{v}_\beta, \quad G_{\alpha\beta}(\mathbf{v}_\alpha) \equiv \int g f_\beta \mathrm{d}^3\mathbf{v}_\beta, \qquad C_{\alpha\beta} \equiv \frac{(Q_\alpha Q_\beta)^2}{4\pi\varepsilon_0^2 \mu^2}, \quad (24)$$

$$\ln \Lambda_{\alpha\beta} = \ln\left(\frac{\lambda_D}{b_0}\right), \qquad b_0 \equiv \frac{Q_\alpha Q_\beta}{4\pi\varepsilon_0 \mu g^2}, \qquad \mu \equiv \frac{m_\alpha m_\beta}{m_\alpha + m_\beta}. \quad (25)$$

Here, the H and G are the first and the second Rosenbluth potential, respectively. These quantities describe the influence of scattering centre of type β on the incoming beam of the particles of type α. The first Rosenbluth potential as well as the first term in the equation (23) correspond to breaking of α by β while the second Rosenbluth potential and the second term correspond to scattering of α due to β. Variable g is a magnitude of relative velocity between α and β $g = |\mathbf{v}_\alpha - \mathbf{v}_\beta|$ [ms^{-1}]. lnΛ is so called Coulomb logarithm and μ is reduced mass [kg]. The equation (23) in this form is suitable for RE description. However, its precision is limited as the derivation of the Rosenbluth potentials is not relativistic [6], [7].

7. Runaway particle

We consider a particle to be in the runaway regime if it is accelerated limitless and therefore it can reach relativistic velocities. For nuclear fusion the most important runaway particles are the electrons so we will focus on them. Such particle can escape from magnetic confinement and reach the inner wall, where it can interact with the matter either through collisional ionisation or excitation (i.e. interaction with electrons) or through bremsstrahlung radiation (i.e. interaction with ions) which case prevails for higher energies and higher atomic numbers. This is not the case of typical energies and tokamak components, which can come into contact with plasma. Indeed, the tokamak walls prevent the RE from getting out of the device, but their energy is transformed mostly into hard X-ray radiation instead and therefore it can cause serious damage. As the RE were observed in JET and Tore Supra tokamaks, they are considered to be one of the biggest problems for further ITER project as well. The worst scenarios predict that the RE can melt kilograms of wall material. This is the reason why they are object of intensive research nowadays.

Runaway particles can be generated by various mechanisms which can be divided into two groups – primary and secondary [6], [13].
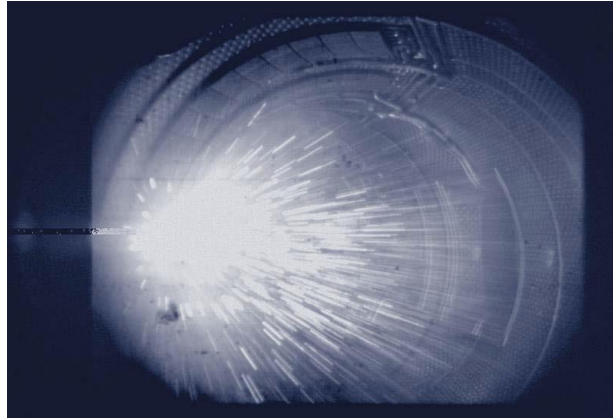

Figure 6: Specks of carbon after RE impact in the chamber of the tokamak Tore Supra [13].

7.1 Primary generation

Let us consider a simple situation, when monochromatic beam α (i.e. constant velocity and concentration) is incoming to a homogenous isotropic Maxwellian plasma target β. The α beam is slowed down to velocity $\mathbf{v}(t)$. No external force field is present. Then the probability density functions are given by Dirac and Maxwell distribution, respectively:

$$f_\alpha = n_\alpha \delta(\mathbf{v}_\alpha - \mathbf{v}(t)), \tag{26}$$

$$f_\beta = n_\beta \left(\frac{m_\beta}{2\pi k_{\mathrm{B}} T_\beta}\right)^{\frac{3}{2}} \mathrm{e}^{-\frac{m v_\beta^2}{2 k_{\mathrm{B}} T_\beta}}. \tag{27}$$

Using these expressions together with equations (23), (24) and (25) we can derive equation for runaway particle. Here we can also neglect the diffusion term as the monochromatic beam exhibits no diffusion. The first Rosenbluth potential is computed using error function ϕ, Chandrasekhar function ψ and using an expansion into the Legendre polynomials:

$$\phi(x) \equiv \frac{2}{\sqrt{\pi}} \int_0^x e^{-\xi^2} d\zeta, \qquad\qquad \psi(x) \equiv \frac{2}{\sqrt{\pi}x^2} \int_0^x \xi^2 e^{-\xi^2} d\zeta, \quad (28)$$

$$\frac{1}{|\mathbf{r}-\mathbf{r'}|} = \sum_{l=0}^{\infty} \frac{\min^l(r,r')}{\max^{l+1}(r,r')} P_l(\cos\theta). \qquad (29)$$
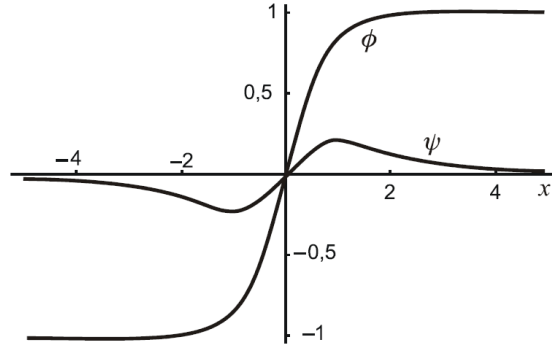
Figure 7: The error function ϕ and the Chandrasekhar function ψ [7].

This expansion is suitable for spherical symmetrical problems as the Coulombic collision of this configuration is. Here, the quantities r, r' are spherical radii with θ an angle between them. P_l are the Legendre polynomials given by

$$P_l(x) \equiv \frac{1}{2^l l!} \frac{d^l}{dx^l} (x^2 - 1)^l. \qquad (30)$$

Now the first Rosenbluth potential is

$$H(v_\alpha) = \frac{n_\beta}{v_{0\beta}} \frac{\phi(x)}{x}, \qquad\qquad x \equiv \frac{v_\alpha}{v_{0\beta}}, \qquad (31)$$

where the quantity x (relative velocity) is used instead of velocity as it can be advantageous to use dimensionless quantities. $v_{0\beta}$ is the thermal velocity of the target [m/s]. Putting it altogether into the Fokker-Planck equation we can derive

$$\frac{\partial \mathbf{v}}{\partial t} = -C_{\alpha\beta} \ln \Lambda_{\alpha\beta} 2 \frac{n_\beta}{v_{0\beta}^2} \frac{\psi \ v/v_{0\beta}}{v} \mathbf{v}, \qquad (32)$$

25

where the magnitude of velocity v is now given by integration over the v_α distribution. We can denote collision frequency

$$\nu_{\alpha\beta} = -C_{\alpha\beta} \ln \Lambda_{\alpha\beta} 2 \frac{n_\beta}{v_{0\beta}^2} \frac{\psi(v / v_{0\beta})}{v}, \tag{33}$$

and considering a weak electric field in the plasma, we can write full equation of motion for the particle

$$\frac{\partial \mathbf{v}}{\partial t} = \frac{Q\mathbf{E}}{m} - \nu(v)\mathbf{v}. \tag{34}$$

Then the particle is either braked or accelerated depending on which one of the terms on the right side prevails.
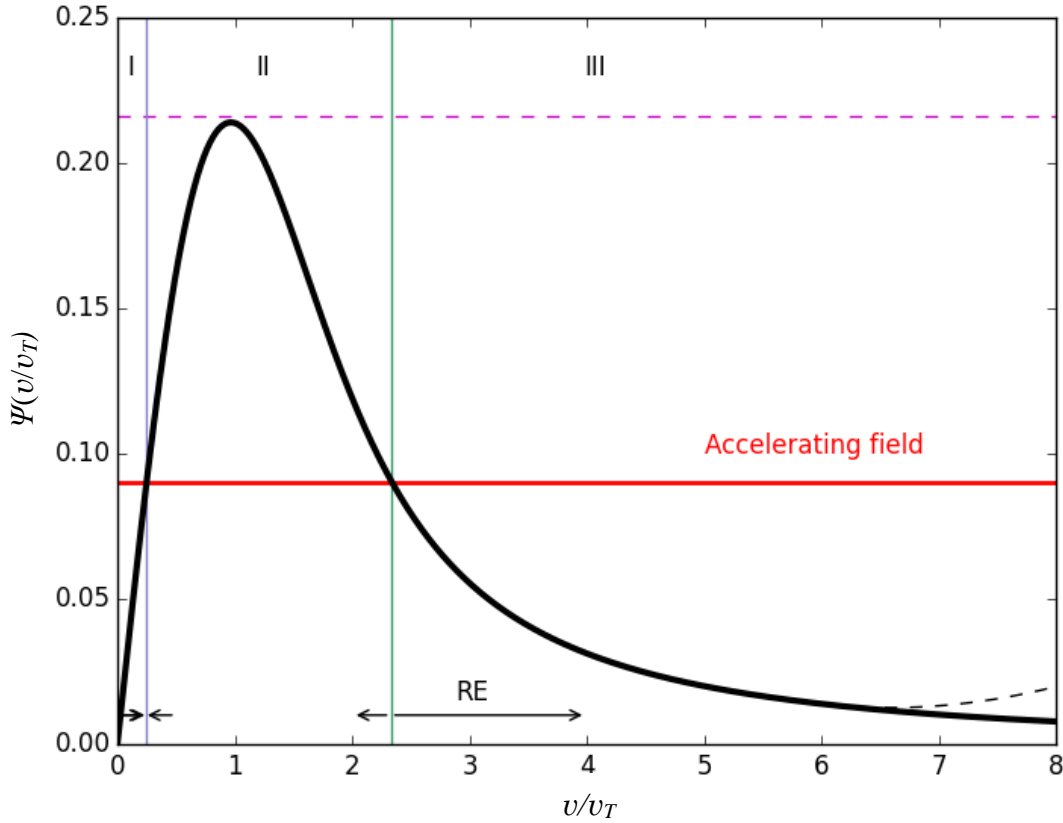

Figure 8: Braked and runaway particle [6].

On the Figure 8 the area **I** corresponds to the situation when the breaking term is smaller than the accelerating term and therefore the particle is accelerated to point given by the vertical blue line. Area **II** is the opposite case and the particle is braked to the point again and hence, this point is stable. Such situation is so called ohmic regime. Area **III** corresponds to so called runaway regime as the particle is theoretically accelerated limitless because of the fact that the breaking term is always smaller than the accelerating term. Hence, the point given by the green vertical line is unstable. The black line is the breaking term in the equation (34). The

black dashed line corresponds to the fact that there is actually a number of channels by which the particle can lose its energy as described below. The peak of the function with the purple dashed line corresponds to so called Dreicer field E_D [V/m] for which all the electrons are in the runaway regime.

$$E_D = \frac{n_e e^3}{4\pi\varepsilon_0^2 k_B T} \ln \Lambda. \tag{35}$$

Here e is the elementary charge [C]. Similarly, we can define co called critical field for which at least some electrons are accelerated.

$$E_c = \frac{n e^3}{4\pi\varepsilon_0^2 m_e c^2} \ln \Lambda. \tag{36}$$

This critical field corresponds to the local minimum of friction force function, which it's minimum for the kinetic energy equal to the rest energy of the particle. However, the real value observed in experiments is higher due to actual temperature dependence. From here it is possible to derive an expression for so called critical velocity very straightforwardly

$$v_c = \sqrt{\frac{n e^3 (1 + Z_{eff} / 2)}{4\pi\varepsilon_0^2 m_e E}}, \tag{37}$$

where the Z_{eff} is the effective nuclear charge [C] and it is a measure of impurities in the plasma. Meaning of the critical velocity is that every particle with the velocity is accelerated to relativistic energies. Situation when the $v_c \rightarrow v_{th}$ (i.e. thermal velocity – mean over the velocity distribution function) means that the Dreicer field is present. The critical velocity can be used for estimation of RE concentration in plasma with the Maxwell distribution.

$$n_{RE} = \int_{v_c}^{c} n_e \left(\frac{m_e}{2\pi k_B T_e}\right) e^{-\frac{m_e v^2}{2k_B T_e}} dv. \tag{38}$$

Despite the fact that the equation is not relativistic the upper bound is chosen as c as for our temperatures the contribution of higher values is negligible. For describing the situation when the electric field is higher than the critical field, quasi-steady state assumption can be taken to account and the Fokker-Planck equation can be transformed into toroidal coordinates, which are better suited for this problem

$$\frac{eE_{\parallel}}{m_e}\left(\frac{\partial f}{\partial v} + \frac{1-\xi^2}{v}\frac{\partial f}{\partial \xi}\right) = \nu_{ee}v_{th}^3\left[\frac{1+Z_{eff}}{2v^3}\frac{\partial}{\partial \xi}(1-\xi^2)\frac{\partial f}{\partial \xi} + \frac{1}{v^2}\frac{\partial}{\partial v}(f + \frac{T_e}{m_e v}\frac{\partial f}{\partial v})\right]. \tag{39}$$

Here $\xi = \cos\theta$ – cosine of the angle between magnetic field lines and the velocity vector of the particle. Solution of the equation (39) is so called Kruskal-Bernstein rate and it has been confirmed numerically. Its integration in time gives the concentration of RE

$$\gamma_{\mathrm{D}} = \frac{\mathrm{d}n_{\mathrm{r}}}{\mathrm{d}t} = k n_{\mathrm{e}} \nu_{\mathrm{ee}} \left(\frac{E}{E_{\mathrm{D}}} \right)^{-3(1+Z_{\mathrm{eff}})/16} \mathrm{e}^{-\frac{E_{\mathrm{D}}}{4E} - \sqrt{\frac{E_{\mathrm{D}}(1+Z_{\mathrm{eff}})}{E}}} . \tag{40}$$

Here k is a scaling factor of order unity. Relativistic correction is then

$$\gamma_{\mathrm{R}} = \gamma_{\mathrm{D}} e^{\frac{-k_{\mathrm{B}}T_{\mathrm{e}}}{m_{\mathrm{e}}c^2}} \left[\frac{1}{8} \left(\frac{E_{\mathrm{D}}}{E} \right)^2 + \frac{2}{3} \left(\frac{E_{\mathrm{D}}}{E} \right)^{3/2} \sqrt{1 + Z_{\mathrm{eff}}} \right] . \tag{41}$$

In tokamak, this mechanism can take place during disruptions e.g. when the plasma is cooled down. As the conductivity of the plasma is proportional to $T^{3/2}$, the cooling process is followed by steep increase of electric field. Then many electrons can get to the runaway regime. Another such situation is so called radiative disruption. It is caused by sudden increase of impurity concentration resulting in loss of conductivity and hence to a quench of current. The impurities can originate from walls of chamber or from intentionally injected high-Z gas or pellets, which are used in order to face the more dangerous disruptions e.g. vertical displacement. It is necessary to mention that the fast electrons are not slowed down during the cooling process as their collisional frequency is small. However, for ITER project the electric fields are rather small (0.1V) and it was proven that in this case the Dreicer mechanism is relatively weak in comparison with secondary generation mechanisms [6], [7].

Let us now mention very briefly some other mechanisms of RE creation, besides the most important one described above. As the tritium is radioactive (with half life time over 12 years) the beta decay can be also a significant source if we take into account longer experiments. However, the energy of such electrons is more or less similar to the energy of thermal electrons in plasma (>20 keV). Another mechanism is the Compton scattering of gamma photons on free electrons. Presence of photons with the energy of MeV in the reactor can be caused e.g. by RE impact on the wall or by some nuclear reactions. Such photons can than interact with the plasma electrons. Also plasma instabilities can be a source of RE [6].
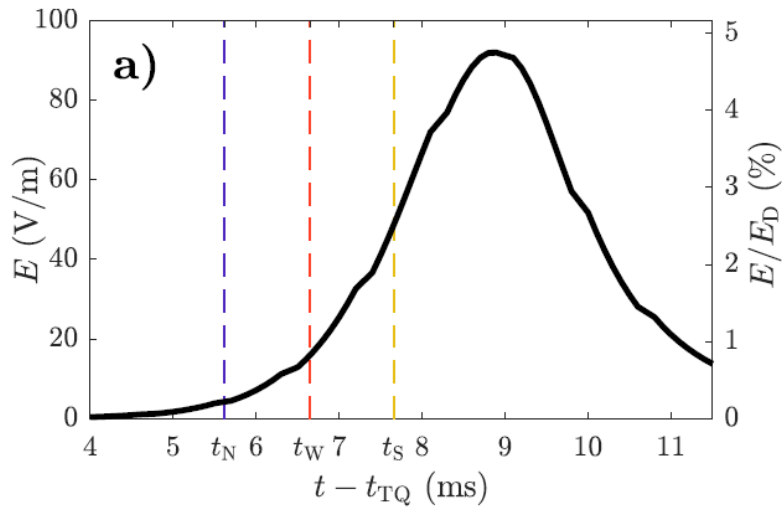

Figure 9: Numerical simulation of electric field during the disruption in ITER plasma [14].

7.2 Secondary generation

Following mechanisms are called secondary as they can take place only if there are already some fast electrons present (seed). Such electrons can establish an avalanche resulting in multiplication of RE population by so called knock-on collisions. These are close collisions (i.e. with small impact parameter b_0) with large amount of parallel momentum being transformed. One RE can push more than one thermal electron to the runaway region while retaining enough momentum to stay in the region itself. So the avalanche mechanism results in increase in RE population but on the other hand also in decrease of average velocity as the energy of secondary RE are around 10-20 MeV for primary RE up to energies of 100 MeV. Equation for secondary generation has been found by Rosenbluth and Putvinski. They used the Fokker-Planck equation with the relativistic right side and they interpolate the solution for relatively wide range of conditions. Relativistic form for the left side of the Fokker-Planck equation has never been found, however, the first and the second Rosenbluth potentials are going to zero for the relativistic energies anyway. The Rosenbluth-Putvinski growth rate of RE due to the avalanche effect is

$$\gamma_{\mathrm{A}} = \frac{\mathrm{d}n_{\mathrm{r}}}{\mathrm{d}t} = \frac{(E-1)n_r}{\tau \ln \Lambda} \sqrt{\frac{\pi \Phi}{3(Z_{\mathrm{eff}}+5)}} \left[1 - \frac{1}{E} + \frac{4\pi(Z_{\mathrm{eff}}+1)^2}{3\Phi(Z_{\mathrm{eff}}+5)(E^2+\frac{4}{\Phi^2}-1)} \right]^{-\frac{1}{2}},$$

$$\Phi(\varepsilon) = \frac{3}{4} \int \frac{2\pi\lambda \mathrm{d}\lambda}{\oint \sqrt{1-\lambda b(\theta)\mathrm{d}\theta}} \approx \left(1 + 1.46\sqrt{\varepsilon} + 1.72\varepsilon\right)^{-1}, \varepsilon \gg 1, \tag{42}$$

$\varepsilon = r/R$ and $E = E_{\parallel}/E_{\mathrm{c}}$. Here, a special system of coordinates is used, namely λ describes the relative role of the perpendicular momentum component and $b(\theta)$ describes the dependency of magnetic field on the poloidal angle θ. The equation can be simplified taking into account limits $E \gg 1$, $Z_{\mathrm{eff}} = 1$ and $\varepsilon \to 0$.

$$\gamma_{\mathrm{A}} \simeq \sqrt{\frac{\pi}{2}} \frac{(E-1)n_{\mathrm{r}}}{3\tau \ln \Lambda} \tag{43}$$

However, such assumptions are not satisfied in present tokamaks, so the simplification is not held in our case.

The avalanching mechanism is in general especially important for small fields, where the Kruskal-Bernstein rate is exponentially small while the avalanche rate is linear. Also, avalanche plays significant role in longer discharges as the rate of RE in plasma is exponential for avalanche but it is linear for Dreicer [5], [6].
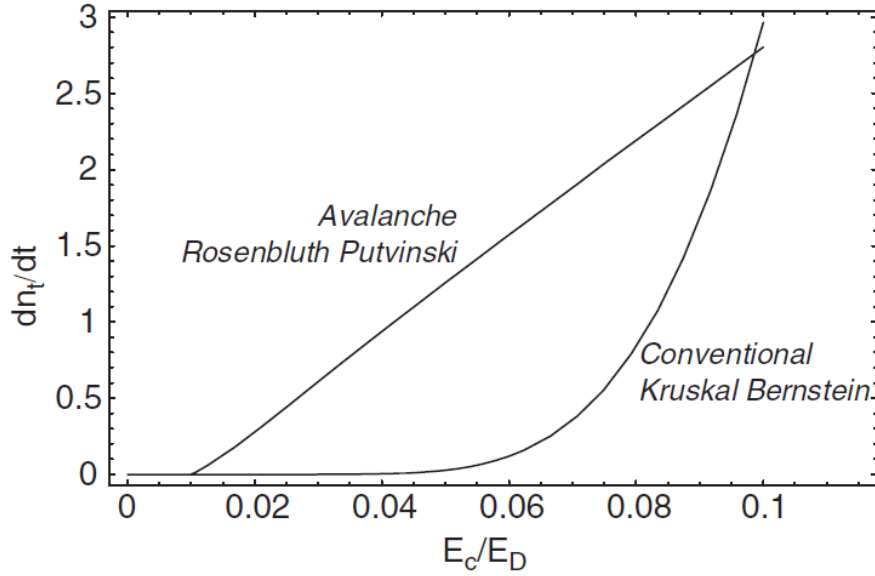
Figure 10: Rosenbluth-Putvinski and Kruskal-Bernstein rate as functions of electrical field [5].

The limits of this description were specified on 2016 by numerical simulation based on kinetic model. It has been shown that for small momentum domain the Rosenbluth-Putvinski theory overestimates the avalanche mechanism for fields when $E/E_c < 10$ and on the other hand it underestimates the effect for fields values $E/E_c > 30$ (i.e. for rather lower temperatures) [15].
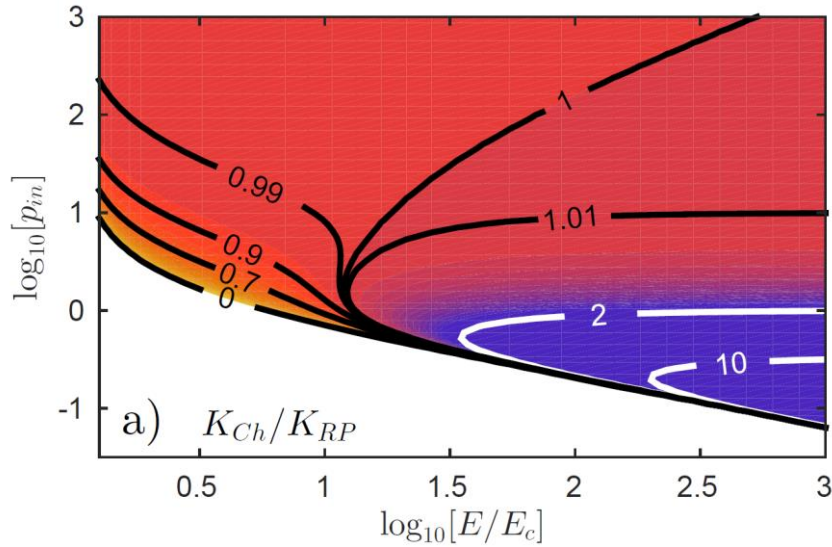

Figure 11: The limits of the Resunbluth-Putvinsky solution. In The orange region, RP operator is overestimating the avalanche generation while in the blue region it is likely to underestimating it [15].

7.3 Runaway losses

We have seen already that the runaway particle can lose its energy by creating avalanches. There are more lose channels as mentioned below Figure 8. Among the other important ones are radiation losses; Bremsstrahlung and synchrotron radiation in particular. Those are very

important for RE detection methods. Last but not least very important channel is electron-positron pair generation. Understanding of these mechanisms is important for ITER project as some effective ways how to mitigate the RE effects on the tokamak have to be found. Let us start with the radiation losses. In general case the dipole radiation power of an accelerated particle is

$$P = \frac{e^2 a^2}{6\pi\varepsilon_0 c^3}.$$ (44)

7.3.1 Synchrotron radiation

Synchrotron radiation is rotation motion of relativistic electrons around the magnetic field lines. It is polarized in plane of the electron path and radiated in the direction of its motion, focused in narrow con. As the polarization is strong, the synchrotron radiation can be used for determination of magnetic field direction. Loss of energy by this channel is in case of RE appreciable for energies above 70 MeV, so this effect is only significant for larger tokamaks, like ITER is. For straight magnetic field lines, the synchrotron radiation power density is

$$P_{\mathrm{cyl}}(\lambda) = \frac{1}{\sqrt{3}} \frac{ce^2}{\varepsilon_0\lambda^3\gamma^2} \int_{\lambda_c/\lambda}^{\infty} K_{5/3}(l)\,\mathrm{d}l,$$ (45)

Where c is speed of light, e is elementary charge, ε_0 is permittivity of vacuum, $K_{5/3}(l)$ is the modified Bessel function of the second kind. $\lambda_c = 4\pi cm_e\gamma_\parallel / 3eB\gamma^2, \gamma = 1/\sqrt{1 - v_\parallel^2/c^2}, B$ is the magnetic field magnitude and finally, m_e is electron mass. Taking into account the tokamak geometry, the expression becomes

$$P_{\mathrm{full}}(\lambda) = \frac{ce^2}{\varepsilon_0\lambda^3\gamma^2} \left\{ \int_0^{\infty} \frac{\mathrm{d}y}{y}(1 + 2y^2)J_0(ay^3)\sin(\frac{3}{2}\xi(y + \frac{1}{2}y^3)) \right.$$

$$\left. -\frac{4\eta}{1+\eta^2}\int_0^{\infty} yJ_0'(ay^3)\cos(\frac{3}{2}\xi(y + \frac{1}{3}y^3)) - \frac{\pi}{2}\mathrm{d}y \right\},$$ (46)

with

$$a = \xi\eta / (1 + \eta^2), \qquad \xi = \frac{4\pi}{3}\frac{R}{\lambda\gamma^3\sqrt{1+\eta^2}}, \qquad \eta = \frac{eBR}{\gamma m_e}\frac{v_\perp}{v_\parallel^2} \simeq \frac{\omega_c R}{\gamma c}\frac{v_\perp}{v_\parallel}. $$ (47)

Equation (46) can be well approximated by (45) for larger tokamaks as the curvature effects become less significant, indeed. Here, R is the major radius, J_0 is the Bessel function. The oscillations of the integrands in the equation (46) make it very difficult to compute. However, taking into account two limits we can get simplifications, which are reasonable in the case of ITER. First of the limits can be summarized as $\eta / (1 + \eta^2) < 1/\eta \ll 1$. Performing the corresponding expansions the equation (46) takes a form

31

$$P_{\text{as1}}(\lambda) \approx \frac{ce^2}{4\varepsilon_0} \sqrt{\frac{2\sqrt{1+\eta^2}}{\lambda^5 R \gamma}} e^{-\xi} \left[I_0(a) + \frac{4\eta}{1+\eta^2} I_1(a) \right]. \tag{48}$$

This approximation is only valid for large normalized momenta. The second limit can be derived for $\lambda \ll (4\pi / 3) R\eta / (\gamma^3 (1+\eta)^3)$. Following simplification has wider validity than (48)

$$P_{\text{as2}}(\lambda) = \frac{\sqrt{3}}{8\pi} \frac{ce^2 \gamma}{\varepsilon_0 \lambda^2 R} \frac{(1+\eta)^2}{\sqrt{\eta}} e^{\frac{4\pi}{3} \frac{R}{\lambda \gamma^3} \frac{1}{1+\eta}}. \tag{49}$$

The description above works very well for single particle, however, in order to obtain correct results, whole RE distribution has to be taken into account.

$$P(\lambda) = \frac{2\pi}{n_{\text{r}}} \int_{\Omega_{\text{RE}}} f_{\text{RE}}(p, \chi) P_i(p, \chi, \lambda) p^2 \, \mathrm{d}p \, \mathrm{d}\chi, \tag{50}$$

where f_{RE} is the RE distribution function, P_i denotes one of the expressions above, n_{r} is RE density, Ω_{RE} is the runaway region of momentum space and $\chi = p_{\parallel} / p = \cos(\theta)$, where θ is the pitch-angle.

The drag force caused by synchrotron radiation is

$$F_s = \frac{2}{3} \frac{e^2}{4\pi\varepsilon_0} \left(\frac{v}{c} \right) \gamma^4 \left\langle \frac{1}{R_c^2} \right\rangle, \tag{51}$$

with average over the field line curvature

$$\left\langle \frac{1}{R_c^2} \right\rangle = \frac{1}{R^2} + \frac{\sin^4 \theta}{r_L^2}. \tag{52}$$

Here r_{L} is the Larmour radius of a particle with its pitch angle equal to θ [6], [17].

7.3.2 Bremsstrahlung

Bremsstrahlung is considered to be the most important loss channel for RE. The word bremsstrahlung originates from German where its meaning is "braking radiation". The origin of this kind of radiation is in decelerating effect of the Coulombic interaction among the charged particles in plasma. Therefore, bremsstrahlung can be understood as a radiation caused by interaction of a charged particle with background. Using Fourier transform of time dependent electric field between the particles, we can obtain the radiation spectra for single electron scattered by ion

$$P(\lambda) = \frac{4\pi}{3} \frac{Z^2 e^6}{m_e c^3 b^2 v^2} e^{-\frac{4\pi cb}{\lambda v}}. \tag{53}$$

Here the quantities have standard meaning. In the case of thermal bremsstrahlung, the frequency range is usually in soft X-ray domain. Then the drag force is [6]

$$F_B = \frac{4}{137} n_e (Z_{\text{eff}} + 1) m_e c^2 \gamma r_e^2 (\ln 2\gamma - \frac{1}{3}),$$

$$r_e^2 = \frac{e^2}{4\pi\varepsilon_0 m_e c^2}. \tag{54}$$

Note, that in comparison with the synchrotron drag force, here we do not have any dependency on magnetic field. On the other hand, eventual impurities have a strong influence. Bremsstrahlung cross-section for fully ionised plasma and electron-ion collision in the relativistic case is given by Bethe-Heitler formula

$$d^4\sigma = \frac{\alpha Z^2 r_0^2}{2\pi} \frac{p \sin\theta \sin\theta_0 \, dk \, d\theta \, d\theta_0 \, d\varphi}{p_0 k q^4}$$

$$\times \left\{ \frac{p^2 \sin^2\theta}{(E - p\cos\theta)^2} (4E_0^2 - q^2) \right.$$

$$+ \frac{p_0^2 \sin^2\theta_0}{(E_0 - p_0\cos\theta_0)^2} (4E_0^2 - q^2)$$

$$- \frac{2p p_0 \sin\theta \sin\theta_0 \cos\varphi (4E_0 E - q^2 + 2k^2)}{(E - p\cos\theta)(E_0 - p_0\cos\theta_0)}$$

$$\left. + 2k^2 \frac{p^2 \sin^2\theta + p_0^2 \sin^2\theta_0}{(E - p\cos\theta)(E_0 - p_0\cos\theta_0)} \right\}. \tag{55}$$

Here $q = |\mathbf{p}_0 - \mathbf{k} - \mathbf{p}|$ is the magnitude of the momentum transferred to the ion. r_0 is the classical electron radius, α is the fine structure constant. All momenta and energies are normalized to $m_e c$ and $m_e c^2$, respectively. θ is defined as an angle between incident (outgoing) electron and the emitted photon. φ is the azimuthal angle between incident electron and outgoing electron. By subscript 0 we understand the incident electron while variables without subscript denote the outgoing electron. In this formula, ion (scattering centre) is considered to be infinitely massive [16].

7.3.3 Electron-positron pairs generation

This quantum electrodynamics effect can take place in electron-thermal ion collisions if the energy of the electron exceeds its rest mass three times, (i.e. ~1.5 MeV). We have seen

already that the energies of the RE are well above this threshold. We can recognize two different cases of this phenomenon.

- Trident process, when an electron emits a photon (i.e. bremsstrahlung) which can in turn generate an electron-positron pair. This process dominates in stronger fields. Production of electron-positron pairs by photons is well known phenomenon which can be written as follows.

$$e^- \rightarrow e^- + \gamma, \gamma \rightarrow e^+e^-, \tag{56}$$

where γ denotes a photon while e^+ and e^- are the positron and the electron, respectively.

- One step process, when the electron-positron pair is generated directly by the electron [18].

$$e^- \rightarrow e^- + e^+e^- \tag{57}$$

Also, the electron-positron pair production can take place in collision between RE and thermal electron if the energy of the RE exceeds its rest mass seven times [19].

Regardless of the way of their birth, the positrons have already high energies and they are accelerated by the field in opposite direction then the electrons are which is in the direction of the plasma current. This makes their motion almost collisionless. Numerical simulations show that the lifetime of the positrons given by annihilation cross section is in order of seconds, giving them enough time to runaway and annihilate on the wall of the tokamak. For example, the number of positrons after the disruption can be estimated as $\sim 10^{14}$, [20] for tokamak JT-60U. This makes tokamak the biggest source of positrons ever made by humans with except of nuclear explosion.

Cross-section corresponding to the direct pair production in the field of nucleus in the relativistic limit is

$$\sigma_{\text{rel}} = \frac{28Z^2\alpha^2 r_e^2}{27\pi} \ln^3 \gamma, \tag{58}$$

Here, Z is charge of nucleus, r_e is the classical electron radius and γ is the Lorentz factor $\gamma = E_0/m_ec^2$, where E_0 is the incident electron energy. The cross-section corresponding to the threshold limit is

$$\sigma_{\text{thr}} = \frac{7Z^2\alpha^2 r_e^2}{2304} \frac{(T_0 - 2mc^2)^3}{(mc^2)^3}, \tag{59}$$

where the T_0 is the incident electron kinetic energy. A fit between the two limits was provided by Gryaznykh in 1998 ($b=10^{-28}$ m^2) [21]:

$$\sigma_{\text{fit}} = 5.22Z^2 \ln^3 \left(\frac{2.3 + T_0 [\text{MeV}]}{3.52} \right) \mu\text{b}. \tag{60}$$
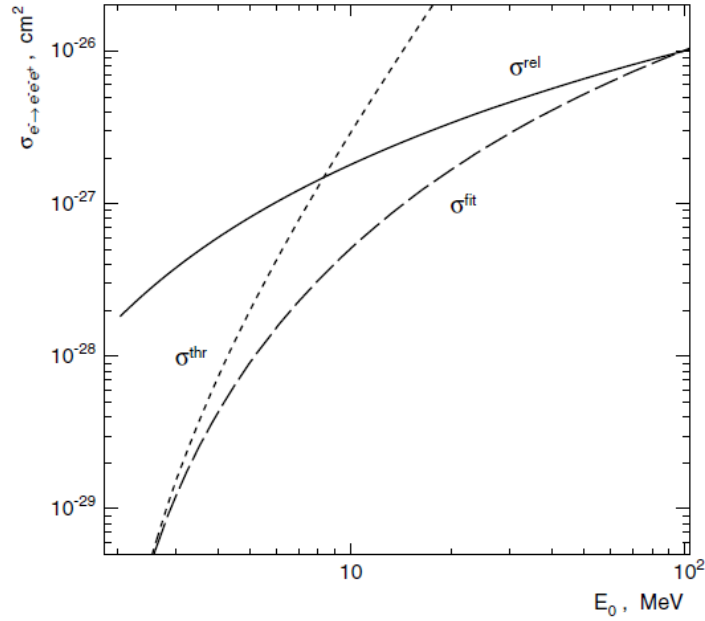
Figure 12: Cross sections for electron-positron pair production by relativistic electron in the field of nitrogen atom [21].

"Total energy of the created electron-positron pair E_e+E_p is simulated according to the differential cross section $d\sigma_{e-\rightarrow e-e-e+}/d(E_e+E_p)$, taken from the formula (30) of Bhabha [1935] for the low-energy limit, formula (34) of Bhabha [1935] for the relativistic case, and interpolation function for intermediate energies."[21].
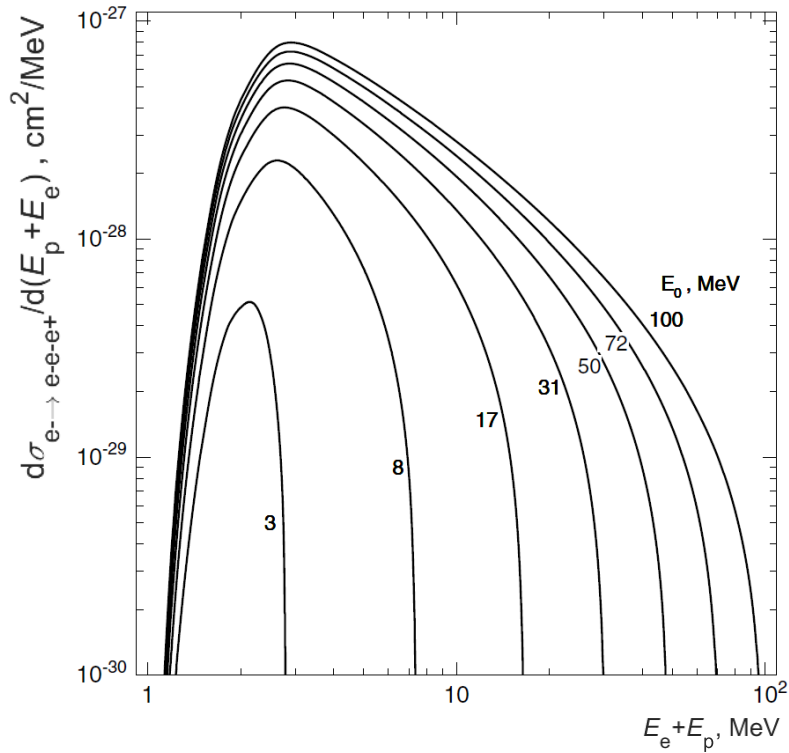

Figure 13: Differential cross section as a function of the total electron-positron pair energy for different incident electron energy E_0 [21].

The energy E_e+E_p is distributed according to the symmetric distribution on Figure 14.
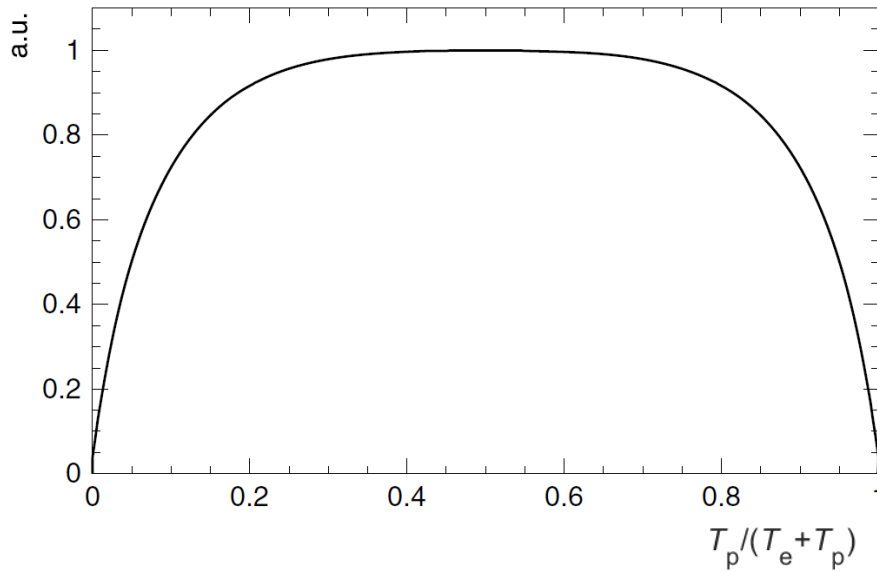

Figure 14: Distribution of total kinetic energy T_e+T_p between created electron and positron [21].

As we can see, the pairs production strongly depends on concentration of impurities, which fact can be eventually used for RE mitigation. Due to presence of bremsstrahlung and other radiation, the detection of the positrons in tokamaks is difficult and it was not successful so far. However, their radiation is peaked in the opposite direction from that of the RE so it may be possible to detect it [6], [22], [23].

7.3.4 Microturbulences

Microturbulences are instabilities in whistler waves, which can occur due to anisotropy in momentum field, resulting in reversion of RE motion. This means that, in principle, it is possible that the pitch angle and energy loss would be enhanced by this effect. Unfortunately, quasi-linear stabilizing mechanism is acting against and according to existing theory it makes the microtubulence contribution to RE losses negligible [24].

7.4 Runaway mitigation strategies

Facing the problem with runaway particles we are not completely helpless. In fact, as intimated above, the physical model of RE gives us certain possibilities. Those strategies are of huge importance as the operational lifetime of ITER project will be very likely set by the runaway mitigation system effectiveness.

7.4.1 Slow cooling

We have seen above, that rapid cooling of the plasma results in steep increase of electric field and then the electrons can reach the relativistic region. Therefore it seems to be very logical to slow down the cooling process in order to avoid such scenario (~40 ms). It can be reached by using so called "killer" pellets, which cool the plasma by radiation. Note that the cooling time is not the same as the plasma current decay time, which depends on electron temperature through the plasma resistivity. It seems that pre-emptive cooling of plasma which is in danger of disruption can be a good option. However, testing of this method is limited by the fact that in the present experimental tokamaks the penetration times for the magnetic field through the walls are different from the case of ITER [24], [25].

7.4.2 Z number increase

The atomic number Z can be increased by delivery of impurities (e.g. argon or neon). As we have seen in the equations (54) and (58) such increase can have a strong influence on the RE loss. Also according to the equations (40) the RE seed generation would be suppressed. Both are indeed advantageous. On the other hand, the average energy of RE is increased, but this effect is expected to be of little importance if the RE current magnitude is reduced exponentially [24].

7.4.3 Suppression of magnetic surfaces

During the discharge in plasma, equilibrium is established as mentioned and so called magnetic surfaces (equipotential lines) are created. During quenching the equilibrium is lost, loop voltage is high and hence the magnetic surfaces are destroyed. Simultaneously, the plasma current decreases due to short circuit caused by RE and a toroidal current is induced to the tokamak walls. However, it is neither sure that all magnetic surfaces are destroyed nor they remain destroyed. It is supposed to be possible to design tokamaks so this toroidal current would provide the suppression of the magnetic surfaces. However, ITER is not designed this way [24].

8. Monte Carlo methods

8.1 Introduction

The Monte Carlo (MC) numerical methods are group of algorithms based on series of random (or pseudo-random) numbers. The first documented application dates back to the end of 40s, although a similar approach has been used by mathematicians since 18th century for multiple integrals computation. It is not surprising that for MC simulations the quality and the speed of the random number generator (RNG) are crucial. The real random numbers can be generated by a piece of hardware using e.g. thermal noise or quantum phenomena. Such a generator can reach very high quality but it's drawback always is that the computations based on it are not repeatable. Therefore, the real random number generators are used for special purposes only. For more common applications (including this thesis) the so called pseudo-random number generators are used instead. Those are based on mathematical algorithms whose period is necessarily finite, meaning that the algorithm repeats the numbers earlier or later. However, if the period is long enough, such generator can provide numbers sequences of high quality. Another problem some worse generators can show is that they do not generate the numbers uniformly but some pattern is present instead. Also, high degree of correlation among the groups of the random numbers can devalue the numerical computations.
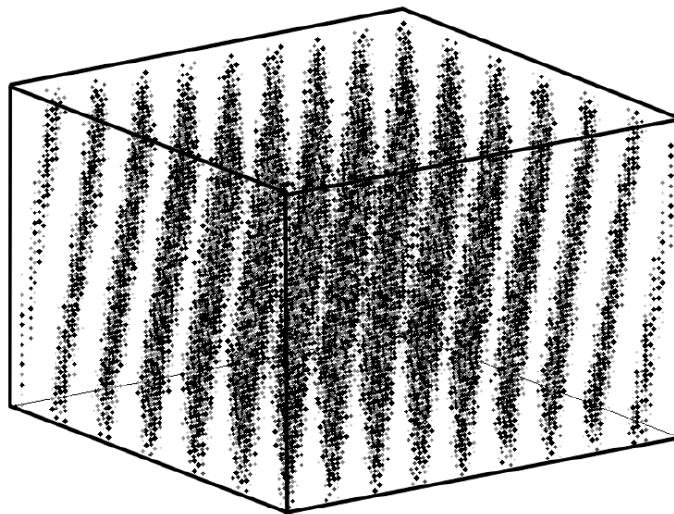

Figure 15: Inappropriate generator IBM RANDU. Obviously, the numbers are generated in 15 planes in 3D cube [7].

8.2 Metropolis method

The method described below is one of the most successful algorithms in history, designed by Nicholas Metropolis, Edward Teller and Marshall Rosenbluth, published in 1953.
For a system in the thermodynamic equilibrium with temperature T we have Boltzmann distribution

$$P_{\text{eq}}(H) = C\,\mathrm{e}^{-\beta H}, \qquad\qquad \beta = \frac{1}{k_{\text{B}}T}, \tag{61}$$

where P_{eq} is probability density and H is energy [J]. Mean values of the dynamical variables takes a form of integration over the phase space:

$$\langle A \rangle = \frac{\int A(S)\mathrm{e}^{-\beta H(S)}\mathrm{d}\Gamma}{\int \mathrm{e}^{-\beta H(S)}\mathrm{d}\Gamma}. \tag{62}$$

Here, the $\mathrm{d}\Gamma$ is an element of the phase space. To find the constant C the partition function has to be computed (i.e. integration/summation over the exponential factors) which is very often impossible to do analytically and not even common numerical methods are capable of finishing such task in a reasonable time in many cases. And here comes the Metropolis method, which can generate so called representative sequence of states S_n with energies $H(S_n)$. If sufficiently high number of sequence members is generated, we can compute the dynamical variable as a simple arithmetic mean, because

$$\langle A \rangle = \lim_{N \to \infty} \frac{1}{N} \sum_{n=1}^{N} A(S_n). \tag{63}$$

The algorithm itself can be described as follows.

1) We choose the initial state of the system. The algorithm generates Boltzmann distribution regardless of the first member of the sequence.

2) Using RNG we generate new state of the system.

3) We accept the new state according to the following rule

$$P_{n \to n+1} = \begin{cases} e^{-\beta \Delta H} & \text{for } \Delta H > 0 \\ 1 & \text{for } \Delta H \leq 0 \end{cases}, \qquad \Delta H \equiv H(S_{n+1}) - H(S_n). \tag{64}$$

4) We proceed to 2).

Here the $P_{n \to n+1}$ is probability of the transition. This means that we always accept a state with lower energy and the state with higher energy we accept with a probability which depends on the difference of energy. This probability-based choice can be also performed using RNG. The algorithm can be used also for temperature dependence examination when performed more times but always with the temperature slightly changed. Also Metropolis algorithm is Markov process (i.e. memoryless). It is also good to mention that the Monte Carlo methods are usually not suitable for computations around phase transitions as the relaxation time is longer here and too high number of sequence members is required. Finally, generalisation of this approach has been found in 1970 by Keith Hastings. Here, the random number $\gamma \in (0,1)$ is generated and we accept the new state if

$$\gamma < \min \left(\frac{P_{\text{eq}}(S_{n+1})P_{n \to n+1}}{P_{\text{eq}}(S_n)P_{n+1 \to n}}, 1 \right), \tag{65}$$

where the $P_{\text{eq}}(S)$ is given distribution [7].

8.3 Realization of continuous random distribution

Using RNG we are generating uniformly distributed points which falls to interval (0,1). In order to generate numbers from a general distribution following algorithm can be used. Having a distribution function $f(x)$ we will define its cumulative distribution function

$$D(x) = \int_{-\infty}^{x} f(x')dx'. \tag{66}$$

It is a monotonically increasing function with limit

$$\lim_{x \to \infty} D(x) = 1, \tag{67}$$

as probability is normalized to one. If we generate random number γ from the interval $\langle 0,1 \rangle$ uniformly, we can write

$$\gamma = D(x) \to x_0 = D^{-1}(\gamma), \tag{68}$$

where x_0 represents our desired value which satisfies distribution $f(x)$.
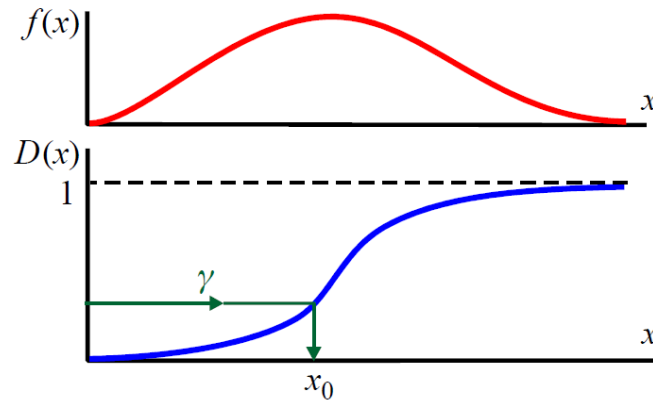

Figure 16: Realization of continuous distribution [7].

Note, that in order to use this algorithm, the inverse cumulative distribution function has to be computed. This is not always feasible and therefore some other algorithm like the one described below has to be used.

8.3.1 Von Neumann method

This method is not as precise as the one described above but it can be on the other hand used in every situation. Having a distribution function $f(x)$ we choose number M so that $M>f(x)$ for every x, where the smaller the M is, the better the method works. Then we generate a random point in rectangular:

$$\eta_1 = a + \gamma_1(b-a),$$
$$\eta_2 = M\gamma_2. \tag{69}$$

Here once again the $\gamma_{1,2}$ are uniformly distributed numbers from the interval $\langle 0,1)$ and a and b determine the range of x-values (see *Figure 16*). The probability is proportional to the area under the curve. Hence, we can use following approach

$$\eta_2 < f(\eta_1) \rightarrow x = \eta_1,$$
$$\eta_2 \geq f(\eta_1) \rightarrow \text{ Generate a new point.} \tag{70}$$

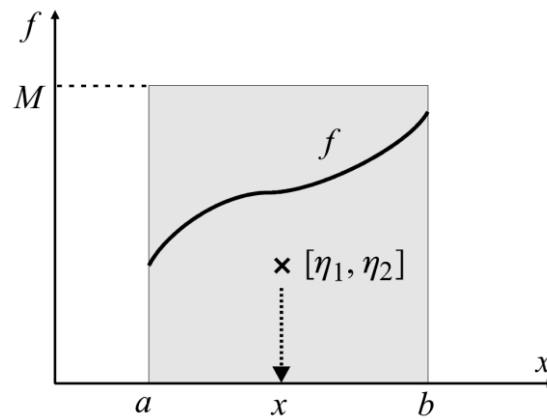This guarantees that the x-values satisfy the desired distribution $f(x)$.

Figure 17: Von Neumann method [7].

8.3.2 Generalized Gauss distribution

In our case we have Maxwell-Boltzmann (MB) distributed particles in the plasma. The one dimensional MB distribution is given by the continues function

$$f(v_x) = \frac{m}{\sqrt{2\pi m k_{\mathrm{B}} T}} \, \mathrm{e}^{-\frac{m v_x}{2 k_{\mathrm{B}} T}} \tag{71}$$

And we know, that Gauss distribution is given by

$$f(x) = \frac{1}{\sqrt{2\pi}} e^{-\frac{x^2}{2}}. \tag{72}$$

This distribution can be generated by the following algorithm. We generate two random numbers from (0,1) interval γ_1 and γ_2. Couple of Gauss distributed values is then [7]

$$
\begin{aligned}
x_1 &= \sqrt{-2\ln\gamma_1}\,\cos(2\pi\gamma_2), \\
x_2 &= \sqrt{-2\ln\gamma_1}\,\sin(2\pi\gamma_2).
\end{aligned}
\tag{73}
$$

And we can notice that the Maxwell and the Gauss distribution differ only by constants. So the equation (73) can be easily generalized and used for MB distributed values generation.

8.4 Diehard tests

As mentioned above, the quality of the RNG is crucial for MC computation. In this thesis I am using RNG provided by Matlab. In order to test its quality I picked following three statistic tests from the Diehard battery [26].

- The minimum distance test.
- The 3D spheres test.
- The parking lot test.

The tests have shown that the RNG generator is sufficient.

9. Runge-Kutta method 4th order

In previous chapters analytical equations of motion for charged particle have been described. However, it is not typically possible to solve any of those equations analytically. The analytical solution is either very difficult to find or – more often – it does not exist at all. Therefore we have to rely on numerical solutions of our differential equations of motion. One very successful and reliable numerical method will be described in this chapter.

Let us assume that we expressed our system behaviour by system of first order differential equations.

$$\frac{\mathrm{d}\xi_k}{\mathrm{d}t} = f_k(t, \xi_1, ..., \xi_n). \tag{74}$$

Here, ξ_k denotes our dynamical variable and $k = 1, ..., n$. Let us consider that we know the solution in time t (initial condition). The Runge-Kutta method is then implemented computing four constants K first:

$$K_{1,k} = f_k(t, \xi_1(t), ..., \xi_n(t)),$$

$$K_{2,k} = f_k(t + \frac{1}{2}\Delta t, \xi_1(t) + \frac{1}{2}K_{1,1}\Delta t, ..., \xi_n(t) + \frac{1}{2}K_{1,n}\Delta t),$$

$$K_{3,k} = f_k(t + \frac{1}{2}\Delta t, \xi_1(t) + \frac{1}{2}K_{2,1}\Delta t, ..., \xi_n(t) + \frac{1}{2}K_{2,n}\Delta t),$$

$$K_{4,k} = f_k(t + \Delta t, \xi_1(t) + \frac{1}{2}K_{3,1}\Delta t, ..., \xi_n(t) + K_{3,n}\Delta t). \tag{75}$$

Here the Δt is so called integration step. Note, that every next constant depends on the previous one so they need to be computed in the right order. Now the solution in time $t + \Delta t$ is

$$\xi_k(t + \Delta t) \cong \xi_k(t) + \frac{1}{6}(K_{1,k} + 2K_{2,k} + 2K_{3,k} + K_{4,k})\Delta t. \tag{76}$$

And the algorithm goes back to its beginning [7].

10. Numerical simulation and results

The main part of this thesis is a Monte Carlo simulation of ultra-relativistic electrons in the plasma. The goal is to examine the influence of electron-positron pair creation on the velocity space of RE. Let us remind here, that also the later generated positrons can reach relativistic energies, being accelerated by electric field in the opposite direction and so they can generate electron-positron pairs themselves exactly the same way as electrons do. Parameters of the plasma and input parameters of the impact particles are expected to be of huge importance and their influence will be discussed in the following text. Before, description of the computational algorithm will be put forward. The simulation is one-dimensional as for the RE electrons the component of velocity in the direction of electric field (i.e. in the toroidal direction if we consider the tokamak geometry) is dominant and important from point of view of eventual damage of the fusion device or mitigation. Nevertheless, the simulating tool is generally possible to use also for plasma in space, where one of the velocity components is also dominant. The simulation does not take into account another energy loosing channels of RE described in chapter 7.3 and instead it focuses on the one particular phenomenon of pairs generation. This restriction allows better precision but on the other hand it came to light that it is not suitable for computations over longer times. The reason is that in the simulation the RE can reach very high energies of GeV after some time which does not happen in real tokamak, as they are slowed down by other mechanisms. Therefore, here the simulation would not match the reality.

The simulation took place in the Matlab computation environment using fourth-generation programming language Matlab. The advantage of this language is its versatility and high level of abstraction and the fact that it contains many useful predefined functions. The biggest disadvantage is its low speed, which appeared to be slightly problematic. The most time demanding part was the Runge-Kutta scheme i.e. the acceleration of the particles in electric field. There were other complex parts of the code e.g. the ones performing the evaluation of generated particles energy, but they were typically called only very rarely.

 On the other hand, this simulation was not very memory demanding.

10.1 Input parameters

The inputs consist of the parameters of plasma and the impact particles (initially electrons only). The parameters of plasma in our model are

- Temperature T [K].
- Concentration of target particles (ions) n_t [m^{-3}].
- Mass of the target particles m_t [kg].
- Toroidal component of intensity of electric field E [V/m].
- Degree of ionization Z [-].
- Coulomb logarithm Λ [-].

The initial impact RE are, as mentioned, ultra-relativistic, which means that their Lorentz factor $\gamma \geq 10$. Besides this beam component of velocity the RE have also chaotic component of velocity given by temperature of the plasma, i.e. by the Maxwell-Boltzmann distribution.

10.2   Computational algorithm

1) Initial beam of electrons creation.
2) Computation of probabilities of pair generation by the impact particles during time step Δt.
3) Decision whether pair has been generated or not.
4) If yes, computation of its energy and the new energy of generating particle. If not, proceed to point 7.
5) Computation of energy of generated positron and electron.
6) Thermalization of the pair particles – addition of chaotic component of velocity. The pair particles then become impact particles.
7) Acceleration of the impact particles according to the relativistic equation of motion (regardless pair was generated or not).
8) Steps 2-7 repeated n-times where n denotes number of time steps Δt to reach the final time of the simulation $t_{\text{final}} = n\Delta t$.

10.2.1 Initial beam of electrons

Having our desired value of Lorentz factor γ of RE (e.g. 10) we can easily compute their beam velocity (in toroidal direction) as

$$v_{\text{b}} = c\sqrt{1 - \frac{1}{\gamma^2}}. \tag{77}$$

Besides the beam component of velocity the RE have also Maxwell-Boltzmann distributed velocity v_{c}, which is determined using algorithm (73). Then we find the resulting initial velocity of impact particle (RE) using relation for relativistic addition of velocity.

$$v_{\text{i}} = \frac{v_{\text{b}} + v_{\text{c}}}{1 + \dfrac{v_{\text{b}} v_{\text{c}}}{c^2}} \tag{78}$$

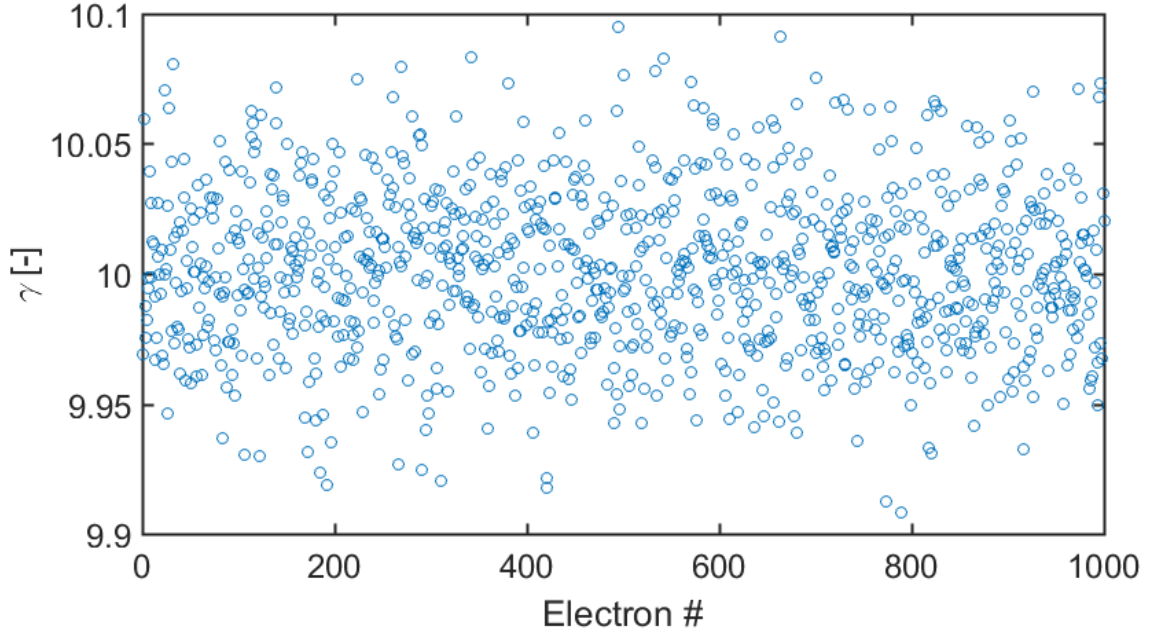As the last step, magnitude of v_{i} is computed.

Figure 18: Velocity space of initial RE population (1000 chosen). As mentioned, their velocity consists of the beam component and the chaotic component. Here the velocity is expressed by Lorentz factor. Indeed, the scattering of the data strongly depends on temperature. Drawn using Matlab.

10.2.2 Probability of creation

Probability of creation of the pair is computed for every of the impact particles. It is performed using equation (60) for cross section as the relativistic kinetic energy can be computed using the velocity (or total energy) from previous step and equation (10):

$$T_i = m_i \frac{1}{\sqrt{1 - \dfrac{v_i^2}{c^2}}} c^2 - m_i c^2. \tag{79}$$

Here, m_i denotes the mass of the impact particle, which is the same for both electron and positron. Once we have the cross section, we can define the probability of creation of electron-positron pair during the time step Δt as

$$\Delta p = \sigma_{\text{fit}} v_i n_t \Delta t. \tag{80}$$

Where σ_{fit} is the cross section from equation (60) and n_t denotes the concentration of the target particles. The equation (80) is valid for small Δt only.

10.2.3 Decision about creation

As a next step the probability from equation (80) is compared with randomly generated number from the interval (0,1). If the generated number is lower than the probability, the electron positron pair is generated. Then the steps described in points 4-6 are performed. If not, we proceed to point 7.

10.2.4 Energy of the generated pair

Knowing the energy of impact particle, we can use

Figure 13 to find the energy of pair generated by the particle. However, the data on the figure are obtained experimentally for some particular energies of impact particle only. In my code I took eleven points on each of the curves and fitted them with appropriate polynomials (fifth or sixth degree). Then it is possible to interpolate between two of those lines according to the value of the actual impact particle energy. For example when energy of the impact particle is 20 MeV, the interpolation between 17 MeV curve and 31 MeV curve is evaluated determining sixty points of the new corresponding curve. The interpolation is performed in both x and y directions. Then, these new sixty points are fitted by polynomial of fifth or sixth degree using the least squares method. Once we have the 20 MeV curve, which represents distribution function in our model, we can use von Neumann method (equations (69) and (70)) for determination of the energy of the generated electron-positron pair.
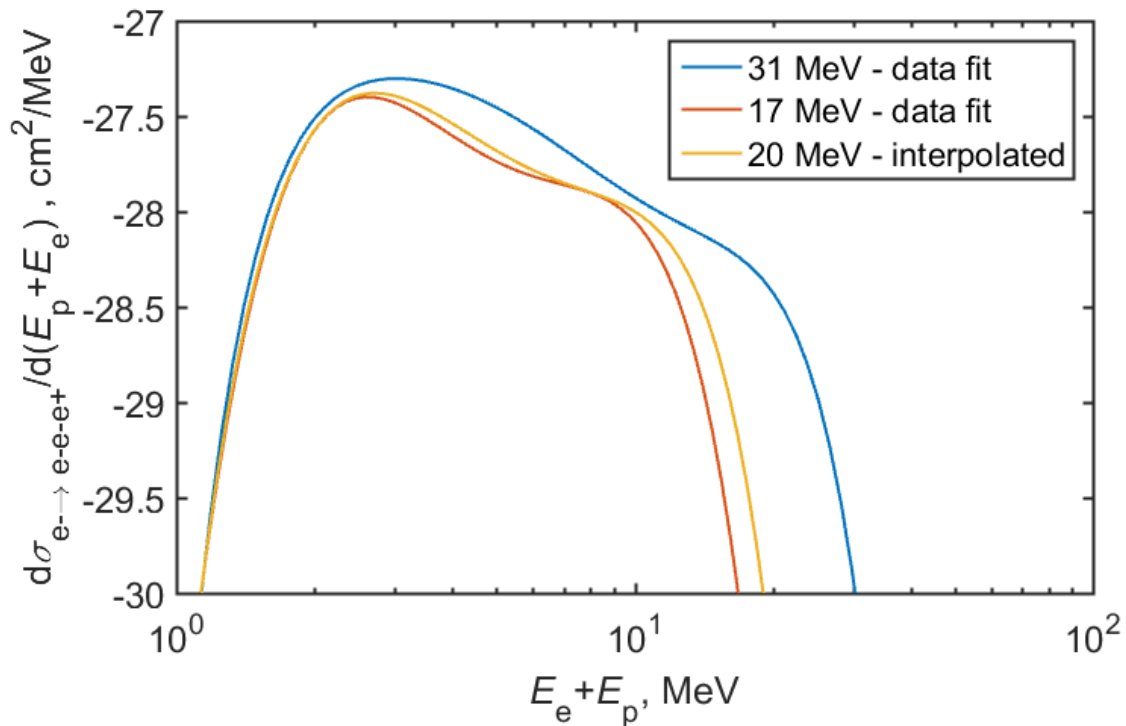

Figure 19: Example of computation of electron-positron pair energy. Drawn using Matlab.

After the generation, indeed, the impact particle loses the energy of the generated pair. The impact particles with energies higher than 100 MeV or lower than 3 MeV are not taken into

account as we have no data for them and therefore it is not possible to estimate their differential cross section of energy for a pair generated by them. However, this simplification seems to be reasonable as particles with higher energies do not usually occur in tokamak and the particles below 3 MeV are not likely to generate any electron-positron pair.

10.2.5 Energy of the generated positron and electron

Once we know the energy of the generated pair, we have to decide about what portion of this energy belongs to each of the two particles. For the task we use distribution function on Figure 14. In my code I used once again approximation by polynomial of sixth degree, which is then used in von Neumann method, which returns the fraction of pair energy associated with the positron. The rest of the energy of the pair belongs to the electron, indeed. The fitting polynomial function found by least squares algorithm takes a form

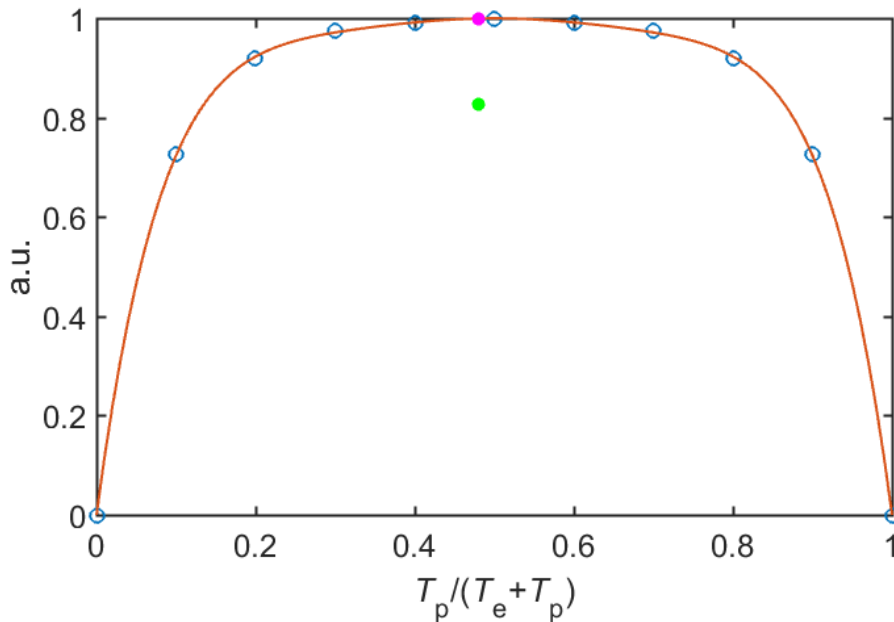$$f(x) = -80.07x^6 + 240.20x^5 - 292.69x^4 + 185.03x^3 - 64.58x^2 + 12.12x. \tag{81}$$

Figure 20: Example of realization of distribution of energy between generated electron and positron. The blue circles are the original data from Figure 20. The red full line is the fitting polynomial (81). Using this probability distribution, von Neumann method is evaluated. In the equation (70) the magenta point corresponds to f(η_1) and the green point corresponds to [η_1, η_2], therefore η_1 is the fraction of the pair energy which pertains to positron. Drawn using Matlab.

10.2.6 Thermalization of the pair particles

To achieve the same conditions for both initial and generated particles in our model, the generated particles are also given a chaotic component of velocity. The component is generated and added to the beam component the same way as in the step 1. The beam component of velocity is indeed computed from energy obtained in the previous step. Once

this step is performed, it is no longer necessary to make a difference between the impact particles and the generated particles, so the electron and positron become impact particles.

10.2.7 Acceleration of impact particles

We already know from the chapter 7 that the charged particles are accelerated in the electrical field and that this acceleration prevails over the breaking term in the range of ultra-relativistic velocities. However, the pair generating particle loses its energy and it can end up in ohmic regime. Such particle is not considered in the simulation anymore and number of such slowed down particles is observed during the simulation. Our equation of motion (34) in the relativistic, one-dimensional case becomes

$$\frac{\partial(\gamma v_i)}{\partial t} = \frac{eE}{m_i} - \nu(v_i)v_i. \tag{82}$$

The second term on the right side is proportional to the Chandrasekhar function (28), which is fairly complicated and so it is replaced by polynomial function in my algorithm. This polynomial function fits very well, especially in the range of high velocities, which we are interested in the most [27].

$$\psi(v_i) \approx g(v_i) = \frac{2v_i}{3\pi^{1/2} + 4v_i^3}. \tag{83}$$

Using this simplification, the computational time required for acceleration of one particle during one Δt decreases by roughly 20%.

The fact that the velocity occurs on both sides of the equation (82) is very unpleasant. Let us remind that $\gamma = f(v)$. Therefore we use a substitution very typical for relativistic computations.

$$u_i \equiv \gamma v_i, \tag{84}$$

after which Lorentz factor becomes

$$\gamma = \sqrt{1 + \frac{u_i^2}{c^2}}. \tag{85}$$

At this point the 4th order Runge-Kutta differential scheme is evaluated. In the scheme (75) our $\xi_1 = x_i$ and $\xi_2 = u_i$. The first simulation equation is therefore

$$\frac{dx_i}{dt} = v_i,$$

The second simulation equation is the equation (82). In both equations v_i is substituted according to (84). Once the differential scheme is evaluated, we give the substitution back.

$$v_i(t + \Delta t) = \frac{u_i(t + \Delta t)}{\sqrt{1 + \dfrac{u_i(t + \Delta t)^2}{c^2}}}. \tag{86}$$

As a very last step new energies of the impact particles are computed using the new velocities and the algorithm is going back to point 2.
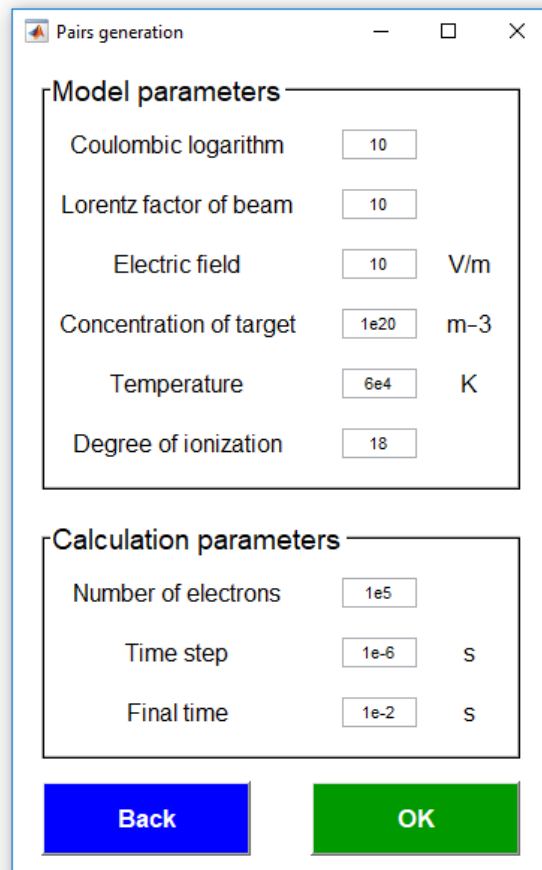

Figure 21: Graphical user interface of the simulating programme.

10.3 Estimations

Before we take a look to the output of the numerical simulation we can try to anticipate the results using the equations which have been put forward above. Let us assume an impact electron whose kinetic energy is $T_0 = 100$ MeV (i.e. upper boundary for our simulation). This assumption gives us the most favourable conditions as the higher the energy of the impact particle the higher the probability of electron-positron pair creation. Also, we can neglect the influence of acceleration and breaking as the particle already has the highest velocity allowed. Considering mitigation by argon i.e. $Z = 18$ the cross section according to the equation (60) is

$$\sigma_{\mathrm{fit}} = 5.22 Z^2 \ln^3 \left(\frac{2.3 + T_0 \left[\mathrm{MeV} \right]}{3.52} \right) \mu \mathrm{b} = 6.48 \cdot 10^{-30} \ \mathrm{m}^2. \tag{87}$$

Then if we consider the time of disruption $\Delta t = 10^{-2}$ s (approximately according to Figure 9) and the concentration of target $n_{\mathrm{t}} = 10^{20} \ \mathrm{m}^{-3}$ we can estimate the probability of pair creation by the impact electron during the disruption time as

$$\Delta p = \sigma_{\mathrm{fit}} v_{\mathrm{i}} n_{\mathrm{t}} \Delta t = 1.94 \cdot 10^{-3}, \tag{88}$$

where the velocity of the impact particle v_{i} is given by its kinetic energy. Based on this result we can expect, that if we repeat the experiment e.g. 100 000 times (which is reasonable number for MC simulation), approximately 200 electron-positron pairs (i.e. 400 particles) will be created. The probability of single pair creation by some of those 400 particles is obviously very small. First, they are very few. Second, they do not exist throughout the simulation and therefore they do not have so much time for the generation and finally third, they do not have in fact such extreme energies we assumed above – the peak of the probability density is 1.5 MeV for generated pair particle! (See *Figure 13*). This could mean that an avalanche of runaway particles cannot be produced by this mechanism during the disruption. Also, we could conclude that this mechanism do not have significant influence on the velocity space of RE population.

With this approach, using the same inputs as Fülöp and Papp used in [22] we will obtain comparable estimation of number of positrons generated in one cubic meter of tokamak during one second i.e. ~$1.5 \cdot 10^{13} \ \mathrm{m}^{-3}\mathrm{s}^{-1}$.

10.4 Disruption simulation

To verify the estimation above, I simulated 100 000 ultra-relativistic electrons for 10 ms with time step $\Delta t = 10^{-6}$ s using the algorithm described in the chapter 10.2. If higher integration step than 10^{-6} s had been used, the simulation would have become unstable – a particle caught in the ohmic regime could be kicked out back to the runaway regime by numerical oscillations. On the other hand with decreasing value of the integration step the time demand of entire simulation increases. The input parameters are chosen according to real conditions in tokamak COMPASS. As mentioned above, the intensity of electric field is changing during the disruption so in order to get as close as possible to the real conditions, following function has been used.

$$E = 1 + 1.6 \cdot 10^7 t^2 \mathrm{e}^{-1000t}. \tag{89}$$

This function resembles the real conditions much better than a single constant value.
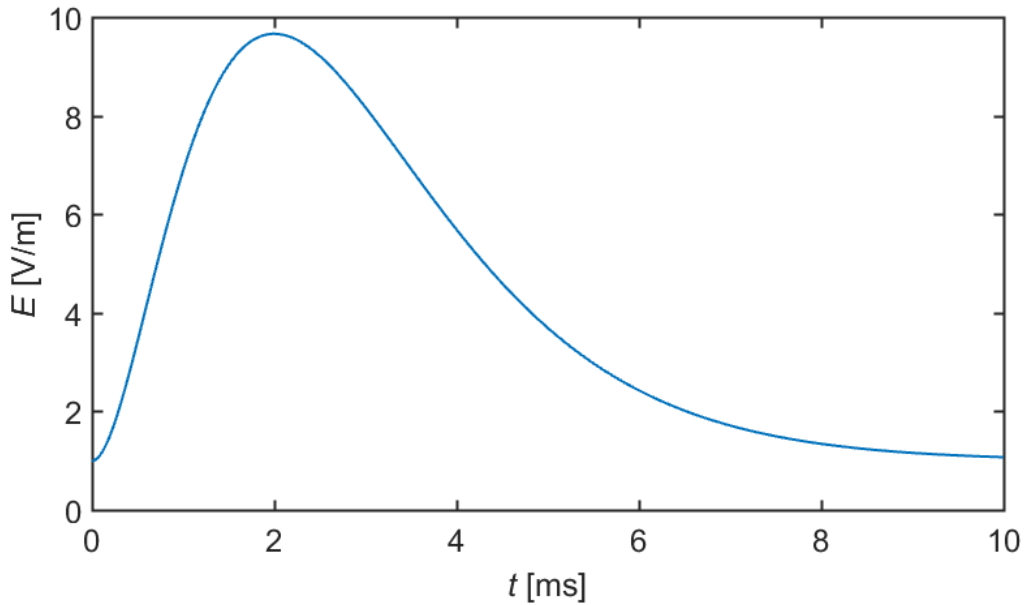

Figure 22: Toroidal component of intensity of electric field used in the simulation of disruption. Drawn using Matlab.

Input	Denotation	Value
Temperature	T [K]	6.00E+04
Concentration of target	n_t [m^{-3}]	1.00E+20
Mass of target	m_t [kg]	1.67E-27
Electric field	E [V/m]	Figure above
Degree of ionization	Z [-]	18
Beam velocity	γ [-]	10
Coulomb logarithm	$\ln \Lambda$ [-]	10

Table 1: Input parameters of disruption simulation. Beam velocity is expressed by the Lorentz factor [28].

The simulation lasted 8450 s and 14 electron-positron pairs have been generated. Comparing with the estimation above, it is a reasonable result when we realize that there we assumed extreme energies of 100 MeV for all impact particles. Here the impact particles had energies the most often slightly lower than 20 MeV. Let us remind here, that the influence of the energy (velocity) of the impact particle on the probability of pair generation is significant as it occurs in computation of the cross-section (logarithmic dependence) and again in computation of probability (v_i).

The impact of these 28 generated particles on the velocity space of the original RE population is therefore completely negligible. Indeed, the generating particles were slowed down, but the slowest one ended up with energy of 9.16 MeV remaining ultra-relativistic. The generated pair particles had typically lower energies as expected, as the peak of probability density of their initial energies is around 1.5 MeV. However, the slowest one ended up with energy of 2.16 MeV which corresponds to velocity of $2.91 \cdot 10^8$ m/s – far from the ohmic regime, which began around $1.35 \cdot 10^8$ m/s for the lowest electric field at the end of the simulation. This result might mean that the electron-positron pairs generation is not significant energy losing channel and therefore it is not useful for RE mitigation. This might seem as a bad news but on the other hand we have to realize that if the pair particles had been more, having high energies they could have become a problem itself.

In order to examine better the influence of the energy of impact particles, a supplementary simulation has been performed. Here, the same parameters has been used but only with 50 000 initial RE and always with different initial beam velocity. The result can be seen on the figure below. The number of generated particles is indeed increasing, but this increase is rather slow.
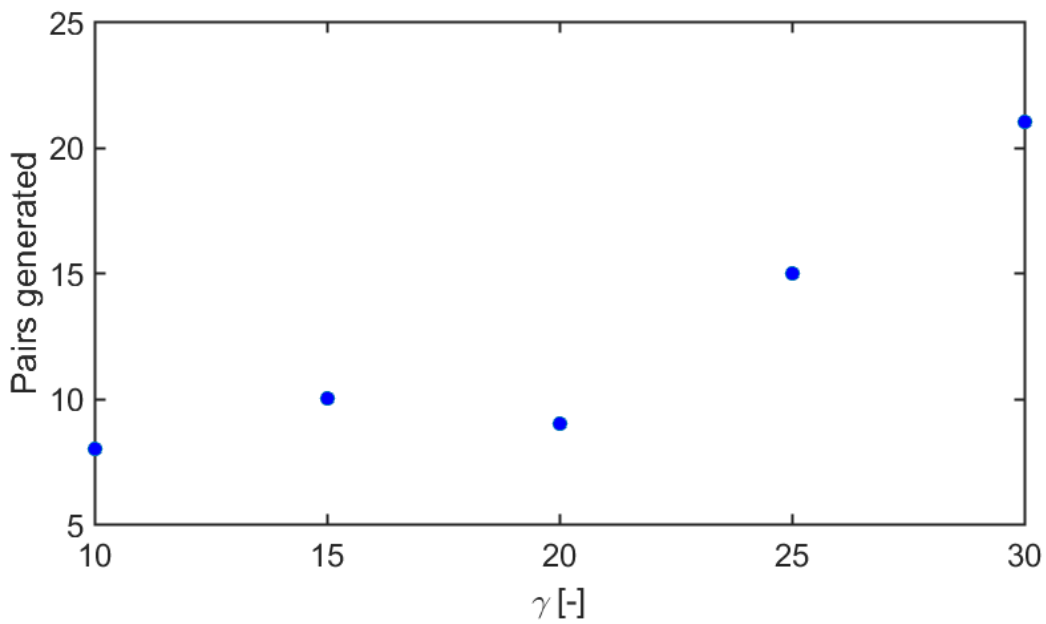

Figure 23: Supplementary simulation examining the influence of the beam velocity on the number of generated electron-positron pairs by population of 50 000 RE. Drawn using Matlab.

As regards the influence of the electric field, it was rather small as can be seen on the *Figure 25*, where we can notice that the energy of the particle did not change drastically due to the acceleration. The electric field plays more important role in shifting the point on the velocity scale where the ohmic regime begins.

Degree of ionization is of huge importance, which is obvious from the equation of the cross section (60). The higher the Z due to impurities or mitigating gas, the more pairs are generated as there is no mechanism acting against. However, I assume in the simulation full ionisation of argon. In reality, only some fraction of the mitigation gas amount is fully ionized

during the mitigation [28]. This means that the number of electron positron pairs produced might be even lower. On the other hand I did not take into account the influence of impurities. Temperature affects the breaking term of equation of motion and therefore it has an influence on the position of the beginning of the ohmic regime. It does not have significant influence on the velocity space, as after the disruption it is very small (see *Figure 18*). Similar influence has the concentration of the target particles, which is once again matter of the impurities and mitigation. In the tokamak COMPASS the concentration of target during the mitigation typically increases by one order [28]. Similarly the Coulomb logarithm affects the breaking term of the equation of motion (with linear law). None of the input parameters with except of the beam velocity and the Z number has a significant impact on the number of generated pairs.
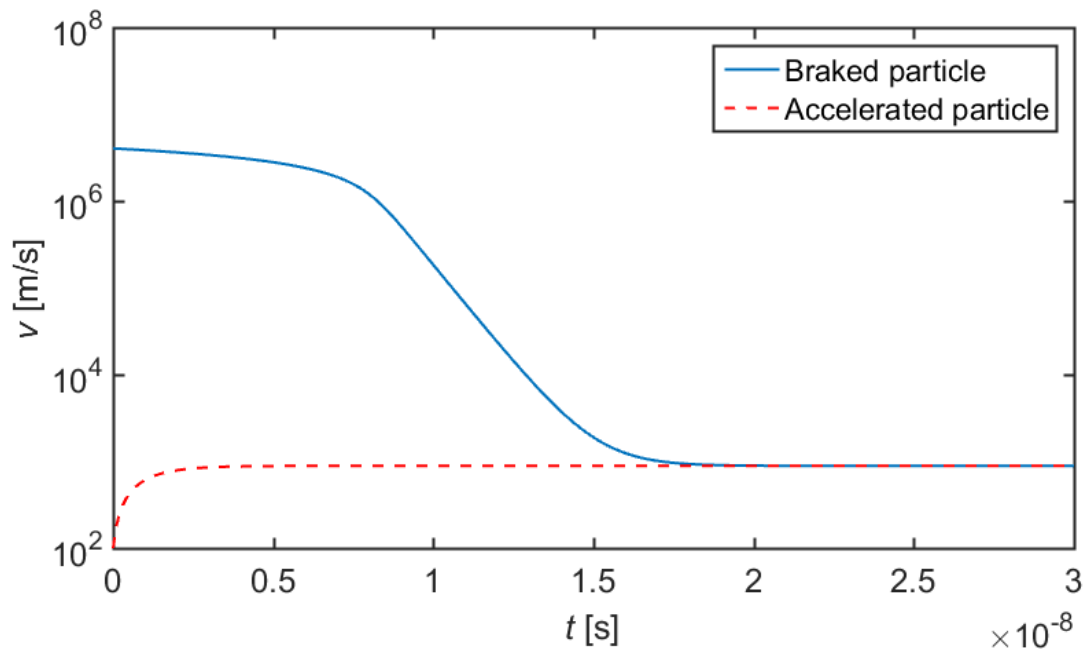

Figure 24: Illustrating figure of braked and accelerated non-relativistic particles in ohmic regime (see also Figure 8). This case however has not taken place during the disruption simulation (i.e. none of the impact particles end up in ohmic regime). Note, that this process is very fast – order of 10^{-8} s – which is much faster than the time scales for relativistic particles as on the figure below. This is because in the non-relativistic region of velocities the difference between braking and accelerating term is huge while on the other hand it is very small in the region of relativistic velocities. Drawn using Matlab.
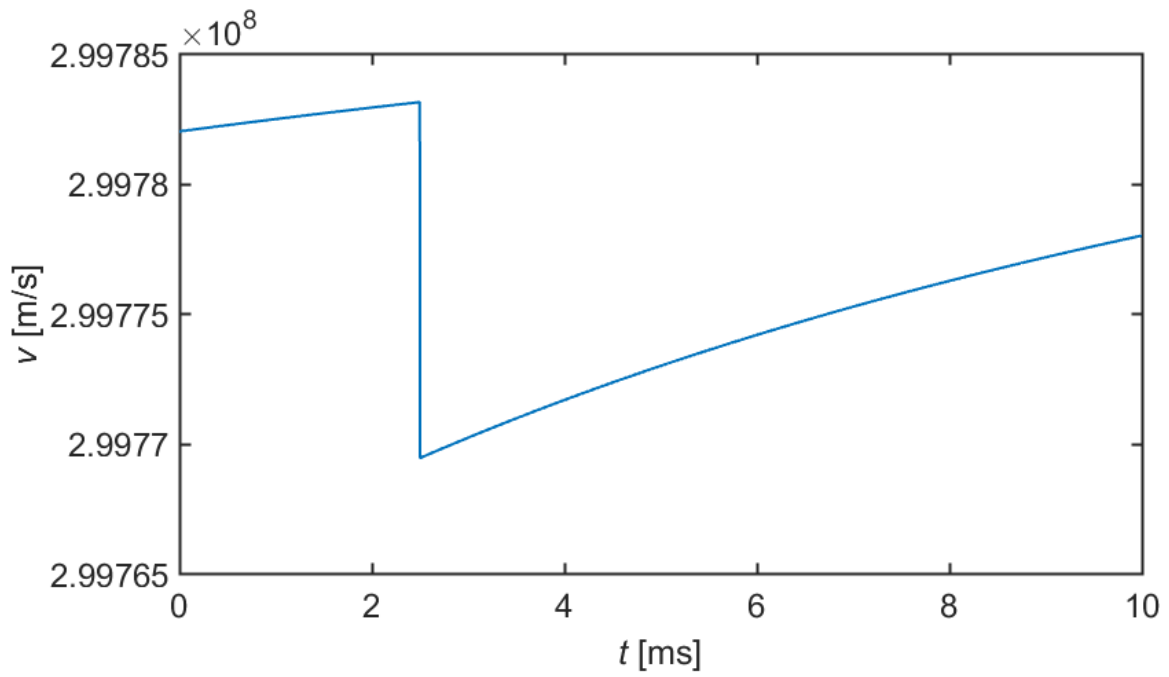
Figure 25: Typical velocity evolution of ultra-relativistic impact particle generating an electron-positron pair in time t = 2.5 ms and therefore losing its energy. The curvature is given by relativistic effects. Drawn using Matlab.

11. Conclusion

In spite of being closer from realization than ever before, the nuclear fusion technology is still facing serious problems and it is far from being commercially implemented. One of the problems is RE which having huge energies can cause serious damage to the inner part of the tokamak chamber. This problem has to be solved long before the first fusion-based power plant will be launched. To make this happened, however, many question still have to be answered.

The first part of the thesis is describing briefly the current fusion technologies and explains what conditions are necessary to run the fusion. Further, the concepts of plasma physics important for understanding of RE are put forward alongside the general description of plasma as a state of matter. First, it is the microscopic description, where we face the problem trying to describe the relativistic particle motion as the current equation of motion gives non-physical solutions which cannot be easily avoided. Second it is the statistical approach examining the collective behaviour of plasma. Here the most important term was the Fokker-Planck equation which described the statistics of the simplified Coulomb collisions in the plasma. From the equation we could derive that for very fast charged particles the accelerating term in their equation of motion can prevails and they can be accelerated almost limitless, giving us the runaway solution. This so called runaway particles is the next chapter focused on, giving the description of first, different ways of their birth i.e. the primary generation and the secondary avalanche mechanism. Second, their different energy losing channels including the synchrotron radiation caused by the relativistic motion, interaction with the background – bremsstrahlung and the quantum phenomena of electron-positron pairs generation, which channel was the most important for this thesis. Third, some possible strategies of RE mitigation have been put forward including slow cooling or Z number increase.

Second part of this thesis is dedicated to the methods and approaches which are later used in the numerical simulation of the RE. Here the most important concept was the Monte Carlo group of methods, which is the family of algorithms based on random numbers and therefore giving statistical results. One of the very important term here was the von Neumann method which allows to realize a random distribution without the necessity of computing the inverse cumulative distribution function. This method was used a number of times later in the simulation. Beside of the Monte Carlo methods, another important algorithm described in this part was the Runge-Kutta numerical scheme, which allows computing the general system of differential equations with high precision and reasonable speed.

Third part of the thesis was as mentioned the numerical simulation. Its main goal was to investigate the influence of the electron-positron pairs generation on the RE population. The simulation has been performed in the Matlab computational environment using its programming language Matlab. Therefore, the first thing which had to be done was the implemented random number generator test. This I performed using the Diehard battery of statistical tests showing that the RNG is sufficient. Later in the chapter, the computational algorithm and approach was described. This part also includes the parameters of the simulation and the input parameters of the plasma, which have been chosen with respect to the real conditions in the Czech ITER-like tokamak COMPASS. The questions I pondered were first, whether the pairs generation has a significant impact on the velocity space of the

original RE population slowing them down and therefore making them less dangerous and on the other hand second, whether the generated particles are becoming ultra-relativistic themselves, being accelerated in the electrical field as well as the original population and hence also becoming dangerous for the tokamak inner walls. Before the actual simulation the estimation has been made. It was based on the same physical model but took into account the extreme, most favourable values for electron-positron pairs production. This way, the influence of this phenomena has been estimated as almost negligible, which result I consider in line with literature and it has been confirmed by the actual simulation. The main part of it lasted more than 8000 s and during the time, 100 000 ultra-relativistic electrons were accelerated in the electric field for 10^{-2} s which time corresponds to typical duration of disruption in tokamak. In every of 10 000 time steps to reach this time period the probability of generating the electron-positron pair has been evaluated. If the pair was generated, its energy has been computed and it was given also the thermal component of velocity. The simulating tool could be handled using graphical user interface.

The results have shown that the velocity space of the original RE population is almost not at all affected by this phenomena and that the new particles are very few in comparison with the original ones. Also, their energies were rather smaller, but still strongly relativistic. The electron-positron production rate was strongly depending on the Z number and the beam velocity while the other input parameters did not play important role. This result would mean that it is necessary to find another ways how to mitigate the existing RE population or completely prevent the RE from being generated.

The validity of the simulation is limited first of all in the time domain. Since it does not contain other energy losing terms, the charged particles would reach huge energies in longer time frame. Such a huge energies would be, however not in line with reality. Another reason is that the positrons are annihilating with the time constant in the order of seconds and the annihilating process is also not included in the computational algorithm. This limitation can be significant as the RE population typically lives a couple of seconds after the disruption.

As mentioned at the beginning of this evaluation, the fusion technology research is far from being done. This thesis is a good example of how difficult it is to predict the future evolution of this field. Here it is possible to state that the research will definitely go on with its intensity unchanged and we can expect that in the following years we will get closer and closer to our desired "box for the star".

12. References

[1] A. FASOLI, "Nuclear Fusion and Plasma Physics, The basics of thermonuclear fusion", *Swiss Plasma Centre, École polytechnique fédérale de Lausanne.*

[2] "60 Years of progress", *ITER*, available at: https://www.iter.org/sci/BeyondITER

[3] "BP Statistical Review of World Energy June 2016", *Centre for Energy, Economics, Research and Policy, Heriot-Watt University* , available at: http://www.bp.com/en/global/corporate/energy-economics/statistical-review-of-world-energy/primary-energy.html

[4] M. ŘÍPA, J. MLYNÁŘ, V. WEINZETTL, and F. ŽÁČEK, "Řízená termojaderná fúze pro každého," *ÚFP AV ČR, Prague*, *2011.* available at: https://www.cez.cz/edee/content/file/vzdelavani/fuze_sceeen.pdf

[5] J. RYDEN, "Monte Carlo simulation of runaway electrons, Master's thesis", *Chalmers university of technology, Göteborg, 2012.* Available at: http://ft.nephy.chalmers.se/JakobRyden_thesis_final.pdf

[6] O. FICKER, "Generation, losses and detection of runaway electrons in tokamaks, Master's thesis", *Faculty of Nuclear Sciences and Physical Engineering, Czech technical university in Prague, 2015. Available at:* http://www.aldebaran.cz/ts/docs_re/2015_Ficker_DP.pdf

[7] P. KULHÁNEK, "Úvod do teorie plazmatu", *Aldebaran group of astrophysics, Prague, 2011.* Available at: http://www.aldebaran.cz/studium/fpla.pdf

[8] K. BARTUŠKA, "*Kapitoly ze speciální teorie relativity*", *1991.* Available at: http://www.ktf.upol.cz/joch/dynamika/kineticka.html

[9] E. POISSON: "An introduction to the Lorentz-Dirac equation", *arXiv:gr-qc/9912045, 1999.*

[10] P.KULHÁNEK, "Vybrané partie z fyziky plazmatu", *Aldebaran group of astrophysics, Prague, 2017.* Available at: *http://www.aldebaran.cz/studium/vkpl.pdf*

[11] M. IBISON, H. E. PUTHOFF, "Relativistic integro-differential form of the Lorentz-Dirac equation in 3D without runaways", *J. Phys. A: Math. Gen. 34, 3421, 2001.*

[12] A. C. M. de OCA, N. G. C. BIZET: „Newton-like equations for a radiating particle", *Phys. Rev. D **91**, 016001, 2015.*

[13] P. KULHÁNEK, "Ubíhající elektrony", Československý časopis pro fyziku, *Prague, 2016.*

[14] A. STAHL, O. EMBREUS, M. LANDREMAN, G. PAPP and T.FÜLÖP , "Runaway-electron formation and electron slide-away in an ITER post-disruption scenario", *arXiv:1610.03249v1 [physics.plasm-ph] 11 Oct 2016.*

[15] A.STAHL, O.EMBREUS, G.PAPP, M.LANDREMAN and T.FÜLÖP, "Kinetic modelling of runaway electrons in dynamic scenarios", *2016.* Available at: https://arxiv.org/pdf/1601.00898.pdf

[16] A.STAHL, O.EMBREUS, G.PAPP, S. NEWTON, E. HIRVIJOKI and T.FÜLÖP, "Effect of bremsstrahlung radiation emission on distributions of runaway electrons in magnetized plasmas", *2015.* Available at: https://arxiv.org/pdf/1511.03917.pdf

[17] A. STAHL, M. LANDREMAN, G. PAPP, E. HOLLMANN, T.FÜLÖP, "Synchrotron radiation from a runaway electron distribution in tokamaks", *2013.* Available at: https://arxiv.org/pdf/1308.2099.pdf

[18] "Pair production in strong fields: The Trident process", *Ludwig-Maximilians-Universität München.* Available at: http://www.theorie.physik.uni-muenchen.de/lsruhl/research/research-ruhl/trident-process/index.html

[19] P. HELANDER and D. J.WARD, "Positron Creation and Annihilation in Tokamak Plasmas with Runaway Electrons", *EURATOM/UKAEA Fusion Association, Culham Science Centre, Abingdon, United Kingdom, 2002.* Available at: http://www.ccfe.ac.uk/assets/Documents/PRLVOL90p135004.pdf

[20] JIAN LIU, HONG QIN, NATHANIEL J. FISCH, QIAN TENG, and XIAOGANG WANG, "What is the fate of runaway positrons in tokamaks?", AIP *Publishing LLC, 2014.* Available at: http://www.aldebaran.cz/ts/docs_re/2014_Liu_positrons.pdf

[21] I. B. VODOPIYANOV, J. R. DWYER, E. S. CRAMER, R. J. LUCIA, AND H. K. RASSOUL , "The effect of direct electron-positron pair production on relativistic feedback rates", *Department of Physics and Space Sciences, Florida Institute of Technology, Melbourne, Florida, USA, 2014.*

[22] T. FÜLÖP and G. PAPP, "Runaway Positrons in Fusion Plasmas", *Department of Applied Physics, Nuclear Engineering, Chalmers University of Technology and Euratom-VR Association, Göteborg, Sweden, 2012.* Available at: http://www.aldebaran.cz/ts/docs_re/2012_Fulop_positrons.pdf

[23] B. KING AND H. RUHL, "Trident pair production in a constant crossed field", *Arnold Sommerfeld Center for Theoretical Physics, Ludwig-Maximilians-Universität München, 2012.* Available at: https://arxiv.org/pdf/1303.1356v3.pdf

[24] A. H. BOOZER "Theory of runaway electrons in ITER: Equations, important parameters, and implications for mitigation", *Department of Applied Physics and Applied Mathematics, Columbia University, New York 10027, USA, 2015.* Available at: http://www.aldebaran.cz/ts/docs_re/2015_Boozer_RE-ITER_PP.pdf

[25] R.W. HARVEY, V.S. CHAN, S.C. CHIU, T.E. EVANS, M.N. ROSENBLUTH, and D.G. WHYTE, "Runaway electron production in DIII–D killer pellet experiments, calculated with the CQL3D/KPRAD model", *Phys. Plasmas. 2000.* Available at: https://fusion.gat.com/pubs-ext/PhysOfPlasma/A23366.pdf

[26] "Diehard tests", Available at: https://en.wikipedia.org/wiki/Diehard_tests

[27] P.KULHANEK, "Runaway electrons behaviour", *2015*.

[28] *Private communication with* O. FICKER, *Czech Academy of Sciences*.